

Atropisomerism about Aryl–Csp³ Bonds: The Electronic and Steric Influence of *ortho*-Substituents on Conformational Exchange in Cannabidiol and Linderatin Derivatives

Hatice Berber,^{†,*} Pedro Lameiras,[‡] Clément Denhez,^{†,⊥} Cyril Antheaume,[§] and Jonathan Clayden^{||}

[†]ICMR, CNRS UMR 7312, Faculté de Pharmacie, Université de Reims Champagne-Ardenne, 51 rue Cognacq-Jay, F-51096 Reims Cedex, France

[‡]ICMR, CNRS UMR 7312, Université de Reims Champagne-Ardenne, Moulin de la Housse, Bâtiment 18, BP 1039, F-51687 Reims Cedex 2, France

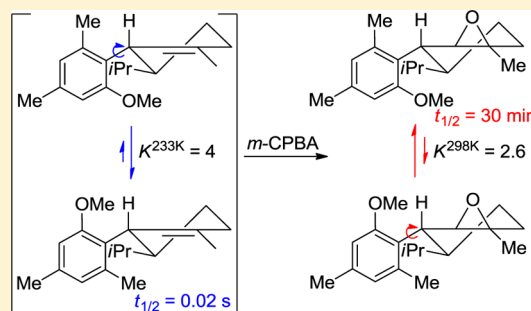
[⊥]Multiscale Molecular Modeling Platform, Université de Reims Champagne-Ardenne, UFR Sciences Exactes et Naturelles, F-51687 Reims Cedex 2, France

[§]Faculté de Pharmacie, Service Commun d'Analyse, 74 route du Rhin, BP 60024, F-67401 Illkirch Cedex, France

^{||}School of Chemistry, University of Manchester, Oxford Road, Manchester M13 9PL, U.K.

Supporting Information

ABSTRACT: Terpenylation reactions of substituted phenols were used to prepare cannabidiol and linderatin derivatives, and their structure and conformational behavior in solution were investigated by NMR and, for some representative examples, by DFT. VT-NMR spectra and DFT calculations were used to determine the activation energies of the conformational change arising from restricted rotation about the aryl–Csp³ bond that lead to two unequally populated rotameric epimers. The NBO calculation was applied to explain the electronic stabilization of one conformer over another by donor–acceptor charge transfer interactions. Conformational control arises from a combination of stereoelectronic and steric effects between substituents in close contact with each other on the two rings of the endocyclic epoxide atropisomers. This study represents the first exploration of the stereoelectronic origins of atropisomerism around C(sp²)–C(sp³) single bonds through theoretical calculations.



INTRODUCTION

Atropisomerism is a stereochemical phenomenon in which hindered single-bond rotation leads to isolable stereoisomers. *Ortho*-substituted biaryls are the most well-known examples where the restricted rotation about C(sp²)–C(sp²) single bonds can generate conformationally separable enantiomers.¹ New methods for asymmetric (atrop-selective) preparation of this compound class still continue to develop.^{1c–h} Recently, the importance of axial chirality has been recognized in drug discovery.² Indeed, biological activity at target molecules such as receptors and enzymes depends on the ability to recognize the active conformer of a conformationally flexible molecule. Remarkable results have been reported in this field³ with a predominant emergence of nonbiaryl atropisomeric compounds such as aryl amides⁴ or aromatic carbamates⁵ in which restricted rotation occurs about an aryl C–N bond.

On the other hand, barriers to rotation about C(sp²)–C(sp³) single bonds are, in general, so small that isomers arising from restricted rotation cannot be separated at room temperature. Nonetheless, in highly hindered systems (when the sp²-hybridized carbon atom is part of an aryl ring with *ortho*

substituents), atropisomers have been isolated.^{1a} In the course of the total synthesis of (–)-linderol A, we prepared endocyclic epoxide intermediates which also display restricted rotation around the aryl–Csp³ bond leading to two unequally populated rotameric epimers with a high rotational barrier between them, of around 80 kJ mol^{–1}.⁶

These compounds happened to be derivatives in the (+)-enantiomeric series of natural products with pharmaceutical or potential therapeutic interests, such as cannabidiol^{7–11} ((–)-CBD) and (±)-linderatins^{12,13} (Figure 1).

Internal rotation of the bond connecting the two rings of cannabidiol was studied by Tamir^{10a} and Ōsawa^{10b} in the 1980s. A brief description^{10a} of an investigation of the conformational properties of (–)-CBD by dynamic ¹H NMR and PCILO calculations suggesting a low rotational barrier for the aryl–Csp³ bond of 28.4 kJ mol^{–1} at 288 K in CDCl₃ was followed by more detailed study in which the conformational behavior of (–)-CBD and its mono- or bis-*ortho*-methoxy

Received: March 14, 2014

Published: June 11, 2014

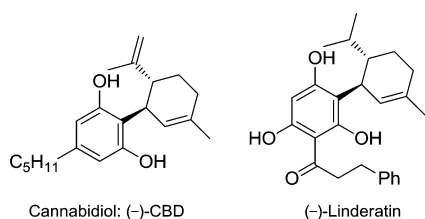


Figure 1. Structure of natural products.

derivatives was investigated by dynamic NMR supported by molecular mechanics at the MM2 level.^{10b} Two major points arise from this study: first, the previously reported low rotational barrier was revised (61.4 kJ mol⁻¹ at 295 K in CDCl₃) to be in close agreement with the recalculated value by Mechoulam (62.7 kJ mol⁻¹ at 288 K in CDCl₃). Second, calculations of model structures showed that phenylcyclohexane derivatives appropriately substituted at β -carbons of the cyclohexane ring (with two methyl groups) and at the *ortho* positions of the phenyl moiety (with two hydroxyl groups) should exhibit atropisomerism.^{10b}

Regarding epoxide derivatives previously reported in the literature, restricted rotation around the aryl-Csp³ bond had never been mentioned, probably due to their symmetrically substituted aromatic ring.^{7,11}

High rotational barriers, resulting in half-lives of at least 1000 s, are required for separation of atropisomers at room temperature. Among the different contributions to the rotational barriers, the bulkiness of the *ortho*-substituents at the axis of chirality plays a dominant role.^{1a,b}

However, there are also results indicating that (stereo)-electronic effects can influence these barriers around C(sp²)-C(sp²) single bonds. Indeed, when an electron-withdrawing group is placed at the aryl moiety excluding *ortho* positions in aromatic carbamates,⁵ significant influence on the rotational barriers induced by the electronic properties of this group has been observed. Conformational analysis in peptoids^{4c,d} has also shown stereoelectronic effects such as intramolecular hydrogen-bonding pattern playing important role in the *cis/trans* equilibrium process. Likewise, conformational analysis in indomethacin derivatives has highlighted stereoelectronic interactions between neighboring substituents at the indole unit and the benzoyl moiety.^{4c} A recent Wilcox molecular torsion balance study has also shown CH- π interactions with rigid side arm which enables the separation of the two atropisomers.^{14a}

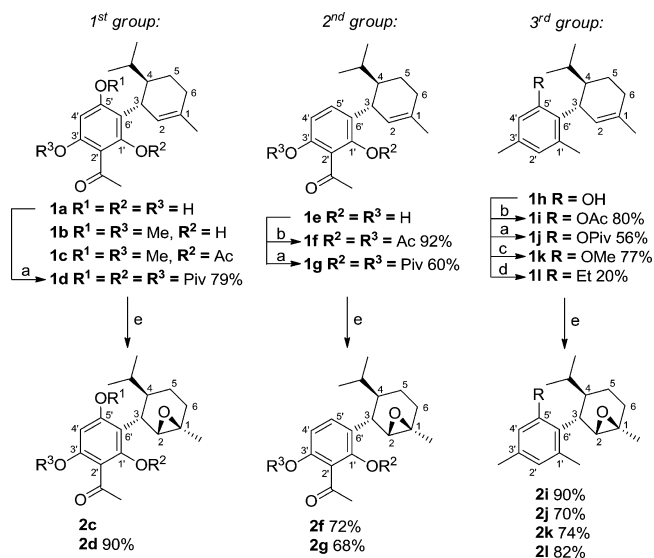
Stereoelectronic effects can even allow the conformation of atropisomeric molecules to be controlled in diaryl ethers^{14b} and in substituted or ring-fused 2-phenylpyridyls.^{1c} The rotational control in these compounds is possible by exploitation of dipolar interactions using sulfoxide substituent at *ortho* position.

In a particular case of C(sp²)-C(sp³) single bonds, π - π interaction influencing the conformation of aromatic rings in isolable atropisomers of 2-arylindoline derivatives has been demonstrated.^{14c} Nevertheless, stereoelectronic effects about C(sp²)-C(sp³) single bonds and specially in cannabidiol remain unexplored due probably to the fact that restricted rotation around such bonds is very rare.

In this paper, we report studies of the influence of steric and/or electronic factors on conformational exchange in some new epoxide derivatives of CBD and comparison with the parent phenylcyclohexene precursors using NMR spectroscopy, with the aim of shedding light on their fluxional properties and thus

generating atropisomeric diastereoisomers (Scheme 1). DFT calculations carried out for three representative compounds (**1c** and **2c,k**) are also described.

Scheme 1. Structure of the Synthesized Compounds^a



^aReagents and conditions: (a) PivCl, py, 80 °C; (b) Ac₂O, py, rt or 80 °C; (c) Me₂SO₄, K₂CO₃, Me₂CO, reflux; (d) (1) Tf₂O, py, CH₂Cl₂, 0 °C; (2) Et₃Al, Pd(PPh₃)₄, THF, reflux; (e) *m*-CPBA, CH₂Cl₂, rt.

RESULTS AND DISCUSSION

Synthesis of Cannabidiol and Linderatin Derivatives.

A useful approach for the synthesis of this class of molecules has been recently reported for **1a-c** and **2c**.⁶ All the investigated compounds displayed in Scheme 1 were prepared starting from a terpenylation reaction between commercially available (-)- α -phellandrene and conveniently substituted phenols. This reaction also provided the monoterpenylated derivatives **1e,h** from the corresponding phenols: 2',6'-dihydroxyacetophenone and 3,5-dimethylphenol, respectively (see the Experimental Section). Then, protection of phenols by esterification conducted to pivalates (or acetates) **1d** from **1a**, **1f,g** from **1e** and **1i,j** from **1h**. The monoterpenylated phenol **1h** was also converted into its methyl ether **1k**. Alkene **1l** with *ortho* alkyl substituents (ethyl and methyl) was also obtained from **1h** in two steps.

Epoxidation of the resulting phenylcyclohexenes (**1d,f,g,i-l**) with *m*-CPBA gave the corresponding epoxide derivatives **2d,f,g,i-l**.

Two major parameters seem to have an influence on the rotation of the aryl-Csp³ bond: the nature (and in particular the bulkiness) of *ortho* substituents, and rigidity of the endocyclic epoxide ring. According to the nature of the *ortho* substituents attached to the phenyl ring, these derivatives were classified into three categories in order to study steric and electronic effects on the conformational exchange process (Scheme 1).

The first group of *ortho* di-O-substituted compounds (with hydroxyl, ether or ester groups) includes alkenes **1a-d** and epoxides **2c,d**. In this type of compounds, steric and electronic factors are associated on both *ortho* positions bearing similar substituents to probe their both effects on the conformational equilibria. Their structures are also interesting because they are

the closest to those of the natural products. However, they differ from the structure of CBD by the asymmetrically substituted aromatic ring which can lead to two conformers.

The second group of *ortho* mono-O-substituted compounds (with hydroxyl or ester groups) includes alkenes **1e–g** and epoxides **2f,g**. This group differs only from the precedent by the nature of one *ortho* substituent. Indeed, one O-substituted group is replaced by a smaller hydrogen atom in order to study the influence of the endocyclic epoxide ring on restricted bond rotation versus *ortho* substituents.

In the last case, we decided to introduce two *ortho* substituents, with at least one sufficiently large to generate observable atropo-diastereoisomeric conformers at room temperature. And specifically, we chose to put a hindered group on one *ortho* position and an O-substituted group on the other *ortho* position to gauge steric effects on one side and electronic effects on the other side. The methyl group seemed to us a sound choice insofar as it is known to have a high steric bulk (van der Waals radius of 2 Å). The other *ortho* substituent was a hydroxyl, ester, ether or alkyl group in alkenes **1h–l** and in epoxides **2i–l**. We also included in this group compounds **1l** and **2l** with alkyl *ortho* substituents as comparison references.

NMR Studies of Conformational Exchange. Eight alkene (**1a–d,i–l**) and eight epoxide (**2c,d,f,g,i–l**) derivatives were chosen for an intensive NMR study (Scheme 1).

Conformational Analysis. In epoxide derivatives **2** (Figure 2), two slowly interconverting conformers (*P*) and (*M*)¹⁵ are detectable at room temperature by ¹H NMR in DMSO-*d*₆. (*P,M*)-**2c,d** were obtained in a ratio of 68:32, respectively. The structure of rotamers (*P*)-**2c,d** and (*M*)-**2c,d** could be identified from the NOESY experiments in DMSO-*d*₆. In the case of rotamers (*P*)-**2d** and (*M*)-**2d**, assignment of the two *ortho* pivaloyl signals was possible from the six resolved signals arising from all the *t*-butyl groups of each rotamer.

Moreover, in the ¹H NMR spectra in DMSO-*d*₆, the C3–H proton is observed at 2.76 and 2.81 ppm in major conformers (*P*)-**2c,d**, respectively and at 3.34 and 2.96 ppm in minor conformers (*M*)-**2c,d**, respectively. This downfield shift, also observed in other solvents (see Table S1 in the Supporting Information), is caused by a deshielding effect of the oxygen lone-pair electrons of the *ortho* O-substituent, meaning that important electronic interactions exist between C3–H and the *ortho* group in front. It is also noteworthy that the deshielding effect observed between conformers of **2c** ($\Delta\delta \sim 0.5$ ppm) with OAc/OMe as *ortho* groups is stronger than that observed for compounds **2d** ($\Delta\delta = 0.15$ ppm) with diester groups (see also Table S1 in the Supporting Information). This could be explained by the decreased electron density on the oxygen atom when the oxygen lone pairs are engaged in delocalization into the carbonyl group, inducing less interaction with C3–H. Furthermore, these observations are in agreement with the structures deduced by NOESY experiments for each conformer of **2c,d**.

The observed stereoselectivity for the formation of the major rotamer (*P*) seems interesting insofar as (*P*)-**2c** is the more polar conformer identified previously by TLC at low temperature.⁶ In accordance with this observation, the dipole moments calculated for **2c** are 9.95 D for (*P*)-**2c** and 6.63 D for (*M*)-**2c** (Table 6 in the computational section).

In the “third group” of compounds, a mixture of two conformers (*M*)-**2i–l** and (*P*)-**2i–l** was also obtained in ratios of 57:43, 24:76, 72:28 and 45:55 in DMSO-*d*₆, respectively. In the ¹H NMR spectra, C3–H proton is observed at 2.96 ppm in

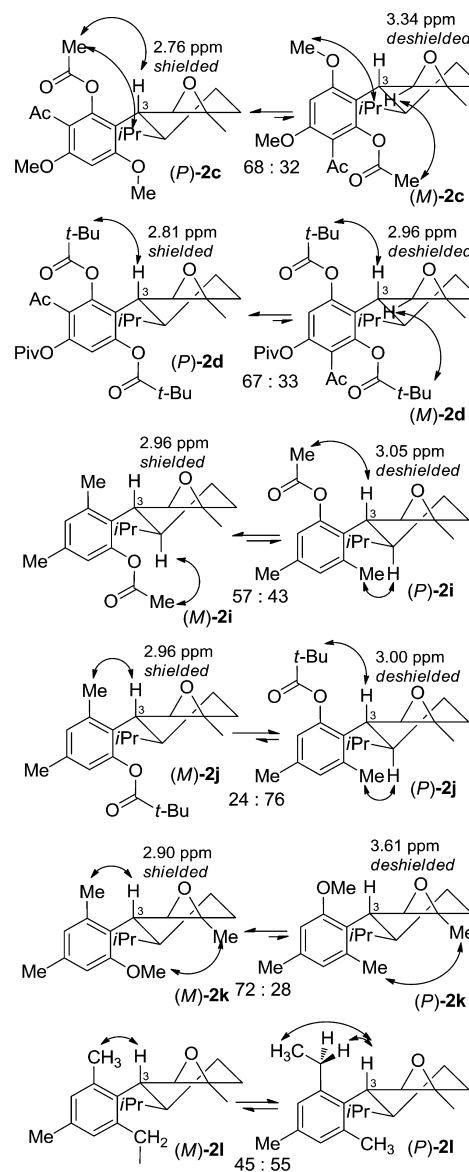


Figure 2. Conformational analysis based on the ¹H NMR spectra and on significant NOESY interactions of epoxides **2c,d,i–l** in DMSO-*d*₆.

both (*M*)-**2i,j** and at 2.90 ppm in (*M*)-**2k**, and at 3.05, 3.00, and 3.61 ppm in (*P*)-**2i–k** respectively, which are in agreement with NOESY results. Likewise, the deshielding effect is in the same range as seen in the “first group” of epoxides **2c,d** with the strongest effect between **2k** conformers ($\Delta\delta \sim 0.7$ ppm).

For the conformers of **2l** (at the bottom in Figure 2), the C3–H proton chemical shift remains unchanged for the two conformers ($\delta \sim 3.1$ ppm), which is not surprising in view of the similar nature of the substituents (ethyl and methyl groups). In the ¹H NMR spectrum, the ethyl group of the major conformer (*P*)-**2l** is an ABX₃ system, while the equivalent signal in the minor conformer (*M*)-**2l** is a simple A₂X₃ (quartet of triplets). As the environment of the ethyl group in interaction with C3–H is chiral, this observation allows us to assign with certainty the stereochemistry of the major conformer, which was also confirmed by NOESY experiments.

Furthermore, **2i–k** appear as two separate spots in each case by TLC at room temperature with different *R_f* values (see the Experimental Section), suggesting that the two conformers interconvert slowly enough to be considered as atropisomers.

The identity of the more polar epimers in **2i,j** was established by analytical HPLC at room temperature (see the Experimental Section and for chromatograms in the Supporting Information): ratios of 67:33 (*M*)-**2i**:(*P*)-**2i** and 27:73 (*M*)-**2j**:(*P*)-**2j** were obtained in 10% EtOAc/hexane. Thus, the more polar epimers turn out to be (*P*)-**2i,j**, which is contradictory in view of the obtained ratios. Indeed the less polar epimer (*M*)-**2i** prevails as expected, while the formation of the major more polar epimer (*P*)-**2j** remains intriguing. The ratios of the peaks on the chromatograms differ elsewhere substantially from those obtained by ^1H NMR, which could probably be explained by the high degree of overlapping peaks associated with a solvent effect.

The identity of the more polar conformer of **2k** was established from dipole moments (see Table 6 in the computational part) calculated for each conformer: 3.62 D for (*M*)-**2k** (the more polar epimer) and 2.63 D for (*P*)-**2k** (the less polar epimer). Here again, interestingly major rotamer (*M*)-**2k** turns out to be the more polar.

Thus, the stereoselectivity in the “third group” of epoxides **2i–k** seems to be governed by electronic effects as seen for the “first group” of compounds (**2c,d**). This aspect is discussed in detail in the next part with the modeled conformers of **2c,k**.

Epoxidation of mono-*O*-substituted arylalkenes **1f,g** (“second group”) gave, to our surprise, epoxides **2f,g** (Scheme 1) showing a single set of NMR signals in each case with broad signals for the benzylic (C3–H) and the neighboring (C2–H) protons. This means that restriction decreased considerably around the C(sp²)–C(sp³) bond rotation even with the endocyclic epoxide, and the presence of two *ortho* substituents is crucial for observation of a mixture of rotamers. VT-NMR experiments were conducted at low temperature and two rotamers appear in a ratio of 76:24 and 95:5 in THF-*d*₈ for **2f** and **2g**, respectively (see entries 3, 4 in Table 2). Unfortunately NOESY experiments at low temperature were unable to discriminate each epimeric rotamer due to the fact that the C3–H and *ortho*-aromatic proton signals were not duplicated.

Alkene derivatives **1** were obtained as single compounds in each case with a very broad signal for the benzylic C3–H proton except for **1l**. The rotation at the CAr–C3 bond is restricted but not enough to observe conformers at room temperature by ^1H NMR. At lower temperature, analysis of proton spectra of alkenes **1a,c,d,i–k** provided interesting results (Figure 3).

Alkene **1a** exists as a 56:44 equilibrium mixture of the rotamers (*P*) and (*M*) at 250 K in MeOH-*d*₃. The individual rotamers (*P*)-**1a** and (*M*)-**1a** could be identified by NOESY experiments. Although NOESY experiments failed at low temperature, rotamers (*P*)-**1c,d** and (*M*)-**1c,d** could be identified with the aid of the chemical shift difference for C3–H protons in the ^1H NMR spectra as observed in epoxide conformers of **2c,d** (see spectra and Tables S1, S2 in the Supporting Information). Indeed, the C3–H proton is observed at 3.82 and 3.45 ppm for major rotamers (*M*)-**1c** and (*P*)-**1d**, respectively, and at 3.28 and 3.55 ppm for minor rotamers (*P*)-**1c** and (*M*)-**1d**. As for epoxide **2c**, the stronger deshielding effect is also observed between rotamers of **1c** ($\Delta\delta \sim 0.5$ ppm). Furthermore, interconversion between di-*O*-substituted conformers (*P*)-**1c** and (*M*)-**1c** led to a ratio of 7:93 at 213 K in THF-*d*₈, which is surprisingly diastereoselective. The observed deshielding effect between (*P*)-**1d** and (*M*)-**1d** ($\Delta\delta = 0.10$ ppm) seems consistent with the similar nature of the *ortho*-*O*-substituents (two pivaloyl groups).

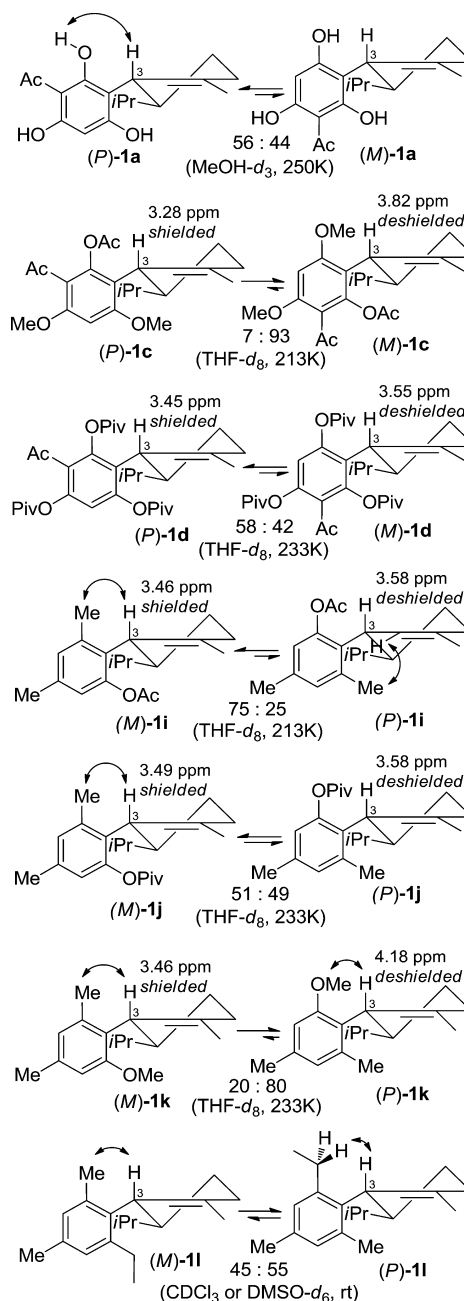
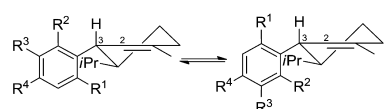


Figure 3. Conformational analysis based on significant NOESY correlations in alkenes **1a,i–l** and on the ^1H NMR spectra of alkenes **1c,d,i–l**.

In this “first group” of *ortho* di-*O*-substituted alkenes **1c,d**, it seems that the origin of the stereoselectivity is more electronic than steric. These stereoelectronic features are discussed in detail in the Computational Studies section with **1c** as model.

For the “third group” of compounds, alkenes **1i–k** showed a single set of NMR signals in each case while **1l** was observed as a mixture of two epimeric conformers (*M*, *P*) on the NMR time scale at room temperature (Figure 3). VT-NMR experiments were conducted at low temperature for **1i–k** and two rotamers (*M*:*P*) become evident in a ratio of 75:25, 51:49 and 20:80, respectively below 233 K in THF-*d*₈. They could be identified by NOESY correlations and by the chemical shift variations of C3–H proton in ^1H NMR spectra. Here again, the stronger deshielding effect is observed between ether conformers of **1k**

Table 1. VT-NMR Studies of Alkenes **1a** (in MeOH-*d*₃), **1b,c,d,i–k** (in THF-*d*₆) and **1l** (in DMSO-*d*₆) at 500 MHz



1a R¹ = R² = R⁴ = OH, R³ = Ac
1b R¹ = R⁴ = OMe, R² = OH, R³ = Ac
1c R¹ = R⁴ = OMe, R² = OAc, R³ = Ac
1d R¹ = R² = R⁴ = OPiv, R³ = Ac
1i R¹ = OAc, R² = R⁴ = Me, R³ = H
1j R¹ = OPiv, R² = R⁴ = Me, R³ = H
1k R¹ = OMe, R² = R⁴ = Me, R³ = H
1l R¹ = Et, R² = R⁴ = Me, R³ = H

entry	compd	coalescing signals	$\Delta\nu^a$ (Hz)	T_c^b (K)	K^c	k_c^d (s ⁻¹)	k_A k_B	$\Delta G^{\ddagger e}$ (kJ mol ⁻¹)	ΔG_A^{\ddagger} ΔG_B^{\ddagger}	$t_{1/2}^f$ (s)	maj (A)	min (B)
1	1a	OH (R ¹)	312	283	1.3	388		55.2		8×10^{-4}		
							494	54.6		6×10^{-4}		
		OH (R ²)	285	283		354		55.4		8.6×10^{-4}		
							451	54.8		7×10^{-4}		
2	1b	OH	151	273	1.1	174		54.9		5×10^{-4}		
							189	54.8		4.5×10^{-4}		
		Har	16	248		18		54.3		6.5×10^{-4}		
							20	54.2		6×10^{-4}		
3	1c	Har	9	243	13	1		58.3		3.4×10^{-3}		
							19	53.1		4×10^{-4}		
		CH ₃ CO	26	253		4		58.6		3.6×10^{-3}		
							56	53.1		4×10^{-4}		
4	1d	Har	39	283	1.4	50		60.0		5.5×10^{-3}		
							69	59.2		4×10^{-3}		
		<u>CHa</u>	210	300		270		59.5		4×10^{-3}		
							373	58.7		3×10^{-3}		
5	1i	Har (R ³)	23	283	3	16		62.7		2×10^{-2}		
							47	60.1		6×10^{-3}		
		Har	24	283		16		62.6		2×10^{-2}		
							49	60.0		6×10^{-3}		
6	1j	Har	46	298	1.0	52		63.2		1.9×10^{-2}		
							54	63.1		1.8×10^{-2}		
		C3–H	32	293		36		63.0		1.8×10^{-2}		
							38	62.9		1.7×10^{-2}		
7	1k	C2–H	53	288	4.0	28		62.6		2×10^{-2}		
							109	59.2		4×10^{-3}		
		Har (R ³)	28	283		15		63.0		2×10^{-2}		
							58	59.6		5×10^{-3}		
8	1l	C2–H	25	343	1.2	31		74.6		1.7		
							37	74.1		1.4		
		Har (R ³)	12	333		14.7		74.4		1.6		
							18	73.9		1.3		

^aChemical shift separation. ^bCoalescence temperature (± 2 –5 K). ^cEquilibrium constant between the two rotamers: A (major) \rightleftharpoons B (minor), where $K = P_A/P_B$. ^dRate constants at coalescence: k_A for A \rightarrow B and k_B for B \rightarrow A. ^eFree energies of activation (± 0.3 –1.1 kJ mol⁻¹) for bond rotation at T_c : ΔG_A^{\ddagger} for A \rightarrow B and ΔG_B^{\ddagger} for B \rightarrow A. ^fHalf-lives for interconversion of rotamers calculated at 298 K assuming $\Delta S^{\ddagger} \approx 0$.

($\Delta\delta = 0.72$ ppm) compared to ester conformers of **1i,j** ($\Delta\delta \sim 0.1$ ppm) as found for **1,2c** and **1,2d** (see also in Tables S1 and S2 in the Supporting Information). It is noteworthy that in the ¹H NMR spectrum of **1k** two broad signals for C3–H are observed at 3.43 and 4.14 ppm in CDCl₃ at room temperature, with a ratio of 25:75.

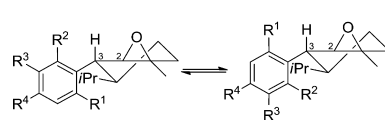
The conformer ratios obtained for acetate and ether rotamers of **1i,k** are surprisingly high and opposite to those of pivalate rotamers of **1j** even though they all bear a methyl group at *ortho* position. Therefore, a steric effect is not sufficient to explain the high diastereoselectivity between conformers in **1i,k**.

Interconversion between (*M*)-**1l** and (*P*)-**1l** with *ortho* alkyl substituents is slow enough on the NMR time scale to allow the detection of two conformers at room temperature in a ratio of 45:55 in DMSO-*d*₆ or CDCl₃ which is interesting because until now no similar alkene derivative has shown this property (Figure 3, bottom). Their structures were identified in a similar manner as the conformers of epoxide **2l** (Figure 2, bottom).

As shown for epoxides **2f,g**, this result confirms that the presence of the epoxide ring is not crucial for generating rotamers on the NMR time scale, unlike the *ortho* substituents which seem to be essential.

Determination of Kinetic and Activation Parameters by VT-NMR Experiments. Dynamic NMR studies were conducted on eight alkene (Table 1) and eight epoxide (Table 2) derivatives at low and high temperatures to help understand the structural features that dictate the dynamics of Ar–Csp³ bond rotation barriers. We applied the Gutowski–Holm equations,^{16a} and/or the graphical method of Shanani–Atidi and Bar–Eli^{16b} (see details in the Supporting Information) to all coalescing signals observed to obtain crude estimates of the rate of Ar–Csp³ bond rotation in these rotamers. Tables 1 and 2 summarize the results of these investigations and give the chemical shift differences between the proton (or carbon) signals which coalesce in the epimeric rotamers (*P*, *M*), their coalescence temperatures and corresponding rate constants, the

Table 2. VT-NMR Studies of Endocyclic Epoxides **2c,d,i–l** (in DMSO-*d*₆) and **2f,g** (in THF-*d*₈) at 500 MHz



2c R¹ = R⁴ = OMe, R² = OAc, R³ = Ac
2d R¹ = R² = R⁴ = OPiv, R³ = Ac
2f R¹ = H, R² = R⁴ = OAc, R³ = Ac
2g R¹ = H, R² = R⁴ = OPiv, R³ = Ac
2i R¹ = OAc, R² = R⁴ = Me, R³ = H
2j R¹ = OPiv, R² = R⁴ = Me, R³ = H
2k R¹ = OMe, R² = R⁴ = Me, R³ = H
2l R¹ = Et, R² = R⁴ = Me, R³ = H

entry	compd	coalescing signals	$\Delta\nu^a$ (Hz)	T_c^b (K)	K^c	k_c^d (s ⁻¹)	k_A k_B	$\Delta G^{\ddagger e}$ (kJ mol ⁻¹)	ΔG_A^{\ddagger} ΔG_B^{\ddagger}	$t_{1/2}^f$ (s)	maj (A)	min (B)
1	2c ⁶	Har	13	370	2.1	20		82.1		32		
			42				79.8		13			
2	2d	CH ₃ CO	10	363	2	15		81.3		24		
			31				79.2		10			
		C2–H	19	378	28		82.8		42			
			57			80.6		17				
3	2f	Har	40	170	3.2	26		58.7		3 × 10 ⁻³		
			82				56.0		1 × 10 ⁻³			
		CH ₃ CO	11	253	7		57.6		2 × 10 ⁻³			
			23			55.0		0.9 × 10 ⁻³				
4	2g	Har	42	275	19	5		63.6		2.5 × 10 ⁻²		
			92				56.8		2 × 10 ⁻³			
5	2i	Har	8	398	1.3	10		90.8		337		
			13				89.8		234			
6	2j	Har (R ³)	8	395	3.2	5		92.3		1814		
			17				88.4		390			
		CH ₃ ortho	8	390	5.5		91.1		1127			
			17			87.2		247				
7	2k	Har CH ₃ O	16.5	408	2.6	13.5		92.3		1700		
			33				89.0		492			
			10.6	403	8.7		92.6		1951			
			21.2			89.4		574				
8	2l	Har (R ³)	3	313	1.2	3.7		73.4		1.1		
			4.5				72.9		0.9			

^aChemical shift separation. ^bCoalescence temperature (± 2 –5 K). ^cEquilibrium constant between the two rotamers: A (major) \rightleftharpoons B (minor) where $K = P_A/P_B$. ^dRate constants at coalescence: k_A for A \rightarrow B and k_B for B \rightarrow A at 298 K. ^eFree energies of activation (± 0.5 –1.3 kJ mol⁻¹) for bond rotation at T_c : ΔG_A^{\ddagger} for A \rightarrow B and ΔG_B^{\ddagger} for B \rightarrow A. ^fHalf-lives for interconversion of rotamers calculated at 298 K by assuming $\Delta S^{\ddagger} \approx 0$.

equilibrium constants between the two unequally populated rotamers, the barriers to Ar–Csp³ bond rotation, and estimates of half-lives for Ar–Csp³ bond rotation at 298 K for both rotamers.

In alkene series (Table 1), ΔG^{\ddagger} values are in the range of 54 to 75 kJ mol⁻¹. Among the different data reported in the literature for cannabidiol (Figure 1) and its monomethyl ether derivative, rotational barriers calculated in acetone-*d*₆ (53.6 and 54.4 kJ mol⁻¹, respectively)^{10b} are the closest values to those obtained for the rotamers of **1a,b** in MeOH-*d*₃ and THF-*d*₈, respectively (entries 1, 2; approximately 55 and 54 kJ mol⁻¹) which possess quite similar structures. Higher bond rotation barriers above 60 kJ mol⁻¹ are obtained for the conformers of **1i–l** (entries 5–8) all bearing one *ortho* methyl substituent. The conformers of **1d** (entry 4) bearing two *ortho* pivaloyl groups also achieve barriers around 60 kJ mol⁻¹. VT-NMR HSQC experiments were also conducted on **1d** (see spectra in the Supporting Information). From the coalescing aromatic carbon signals, we also deduced kinetic parameters for the rotamers of **1d** which are in good agreement with those obtained from coalescing proton signals. Barriers above 70 kJ mol⁻¹ are reached for conformers of **1l** (entry 8) bearing two *ortho* alkyl groups which are known to be sterically hindered substituents. On the other hand, higher diastereoselectivities with equilibrium constants of 13, 4, and 3 were obtained for **1c**, **k**, and **i** respectively (entries 3, 7 and 5). Therefore, a

combination of OMe/Me as *ortho* substituents in conformers of **1k** shows the highest diastereoselectivity and ΔG^{\ddagger} values (best correlation).

In epoxide series (Table 2), ΔG^{\ddagger} values are in the range of 55 to 92 kJ mol⁻¹. The highest bond rotation barriers above 90 kJ mol⁻¹ with half-lives sufficiently higher than those required for atropisomers (or near-atropisomers) are obtained for **2i–k** (entries 5, 6, 7) bearing a bulky methyl and an ester or ether O-substituent. Interconversion between atropisomers of **2j,k** has both the highest stereoselectivities and barriers, meaning that the combination of Me/OPiv or Me/OMe as *ortho* substituents lead to atropisomers (*M*)-**2j,k** and (*P*)-**2j,k** favoring one of the two epimers. Barriers around 80 kJ mol⁻¹ were found in rotamers of **2c,d** (entries 1 and 2) bearing two O-substituents. The increase of about 10 kJ mol⁻¹ from **2c,d** to **2i–k** is therefore due to the hindrance of the methyl group larger than the others. Surprisingly, barriers found between epoxide conformers of **2l** (entry 8) and those of **1l** (Table 1, entry 8) are in the same range, which confirms that in the case of alkyl groups in the *ortho* positions the presence of the epoxide ring does not influence the rotation about the indicated C–C bond. It is also noteworthy that the barriers increased (about 23–29 kJ mol⁻¹) from the parent alkenes **1c,d,i–k** to the corresponding endocyclic epoxides **2c,d,i–k**. This means that for these compounds with at least one *ortho* O-substituent the presence of the epoxy moiety influences the barriers

significantly. Lower barriers of around 60 kJ mol^{-1} were obtained for mono-O-substituted endocyclic epoxides **2f,g** (entries 3 and 4). Indeed, barriers decreased considerably over other epoxides confirming the importance of the two *ortho* substituents. Comparison between **2g** and **2d**, which differ only in the nature of one *ortho* substituent R^1 (H and OPiv, respectively), shows a significant decrease of barriers (around 20 kJ mol^{-1}). Moreover, the equilibrium constant for **2g** is substantially higher ($K = 19$) than others, which is probably due to the bulkiness of the *ortho* pivalate group versus H atom.

The ΔG^\ddagger values were also determined for (*M*)-**1c**, (*P*)-**2c** and (*M*)-**2j** from the Eyring plots of the corresponding rates of interconversion k obtained by line-shape simulation (Table 3),

Table 3. Activation Parameters of Alkene **1c and Epoxide **2c,j** Conformers by Line Shape Simulation at 298 K**

entry	compd	k (s^{-1})	ΔH^\ddagger (kJ mol^{-1})	ΔS^\ddagger ($\text{J K}^{-1} \text{mol}^{-1}$)	ΔG^\ddagger (kJ mol^{-1})	$t_{1/2}$ (s)
1	(<i>M</i>)- 1c ^a	241	60.6	4.5	59.3	4×10^{-3}
2	(<i>P</i>)- 2c ^a	4×10^{-2}	78.7	-13.8	82.8	25
3	(<i>M</i>)- 2j ^b	3×10^{-3}	88.7	-3.8	89.8	333

^aFrom Eyring plot and rate constants k_A for A (major) \rightarrow B (minor).

^bFrom Eyring plot and rate constants k_B for B (minor) \rightarrow A (major).

including the activation enthalpies (ΔH^\ddagger) and entropies (ΔS^\ddagger).¹⁷ We found that this method gives ΔG^\ddagger values that match those from the coalescence temperature measurements described above in Tables 1 and 2. Table 3 shows also that ΔS^\ddagger values are near zero, in the range of 4.5 to $-13.8 \text{ J mol}^{-1} \text{ K}^{-1}$. The dominating activation-enthalpy terms clearly point to a free-energy barrier arising primarily from potential energy constraints for achieving the transition state. It is also noteworthy that the sign of entropy of activation ΔS^\ddagger calculated for alkene conformer (*M*)-**1c** ($\Delta S^\ddagger > 0$, which also is in agreement with the previously recalculated value for CBD by

Mechoulam^{10b}) and epoxide conformers (*P*)-**2c** and (*M*)-**2j** ($\Delta S^\ddagger < 0$) is opposite, indicative of highly organized transition state in endocyclic epoxides unlike more flexible alkene derivatives. The discussion is further developed in the next part with the computed models.

Computational Studies. Alkene **1c** and epoxide **2c,k** derivatives were selected as representative structures for theoretical investigations. The first step involved molecular mechanics exploration of their conformational space, which for each compound provided initial geometries of the local minima using MacroModel software implemented in Schrödinger suite 2013. The conformations were then subjected to a further full geometry optimization in solution in THF for **1c** and in DMSO for **2c,k** using DFT methods implemented in Gaussian09 program at the IEFPCM/M06/6-31G** level of theory.¹⁸ All stationary points (minima, transition states) were properly characterized by frequency calculations using the same DFT methodology. Transition states were identified using the synchronous transit-guided quasi-Newton method (STQN) and optimized using the Berny algorithm at the IEFPCM/M06/6-31G** level of theory.¹⁹ In the second step, accurate estimations of energies of minima and transition states were obtained through single point MP2 calculations at the IEFPCM/MP2/6-31G**/M06/6-31G** level (see the Supporting Information for full structural parameters). The structures of the lowest-energy conformers (minima) and transition-state structures detected for **1c** and **2c** are shown in Figure 4, including energetic barriers (ΔE^\ddagger and ΔE°) at the MP2 level). In alkene conformers of **1c**, the computed barriers agree well with those determined by VT-NMR experiments (Table 1, entry 3 and Table 3, entry 1). In epoxide conformers of **2c**, the computed values, although slightly higher than those obtained experimentally, remain close to them (Table 2, entry 1 and Table 3, entry 2).

Table 4 reports the complete computed energetic parameters of **1c** and **2c,k** conformers. In terms of relative energy between conformers, (*M*)-**1c** was calculated to be the major conformer at 298 K with a ΔG° of 11.2 kJ mol^{-1} (6.4 kJ mol^{-1} at the MP2

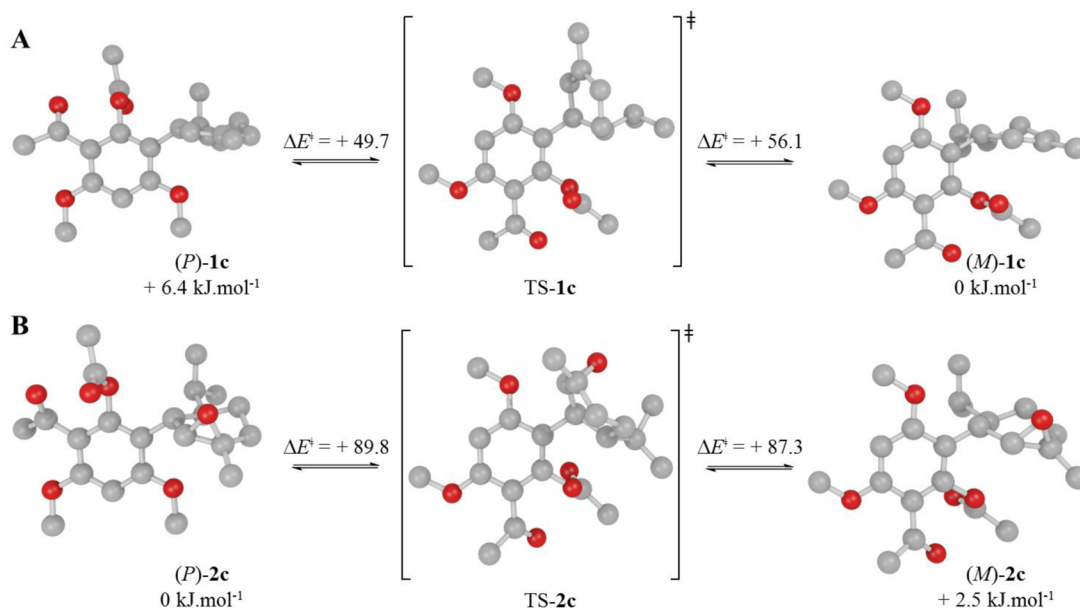


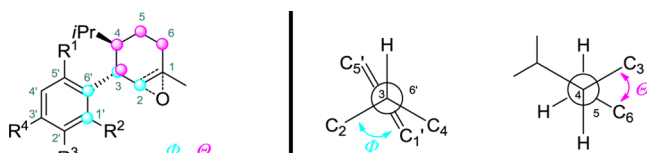
Figure 4. Structures and activated energies (kJ mol^{-1}) associated with the epimerization pathway between (*P*)-**1c** and (*M*)-**1c** through TS-**1c** (A) and between (*P*)-**2c** and (*M*)-**2c** through TS-**2c** (B) calculated at the IEFPCM/MP2/6-31G**/M06/6-31G** level of theory.

Table 4. Computed Energetic Parameters of 1c and 2c,k Conformers at 298 K

compd	$\Delta G^{\ddagger a,b}$	$\Delta H^{\ddagger a,b}$	$\Delta S^{\ddagger c}$	$\Delta G^{o a,b}$	$\Delta E^{\ddagger a,d}$	$\Delta E^{o a,d}$
(P)-1c	57.2	56.3	-2.32	11.2	49.7	6.4
(M)-1c	68.3	64.3	-13.1	0	56.1	0
(P)-2c	94.8	87.1	-25.8	0	89.8	0
(M)-2c	93.3	87.7	-18.9	1.45	87.3	2.5
(P)-2k	101.8	102.1	0.07	11.4	93.3	7.9
(M)-2k	113.2	104.8	-2.5	0	101.2	0

^aEnergies in kJ mol^{-1} . ^bEnergies determined using single point calculations at the IEFPCM/M06/6-31G** level of theory. ^cActivation entropy in $\text{J K}^{-1} \text{mol}^{-1}$ derived from $\Delta G = \Delta H - T\Delta S$. ^dEnergies determined using single point calculations at the IEFPCM/MP2/6-31G** level of theory.

level) versus (P)-1c. Surprisingly, the minor conformer for 2c is featured by (M)-2c with a ΔG^o of 1.45 kJ mol^{-1} (2.5 kJ mol^{-1} at the MP2 level) versus (P)-2c. This inversion in the major conformers between 1c and 2c seems to come from stereoelectronic effects arising from the epoxy moiety. In conformers of 2c, (P)-2k was found to have higher energies ($\Delta G^o = 11.4 \text{ kJ mol}^{-1}$ and $\Delta E^o = 7.9 \text{ kJ mol}^{-1}$) than the more stable (M)-2k. The calculated energetic differences between these conformers are entirely in accordance with ratios determined by $^1\text{H NMR}$. Likewise, the computed values for ΔG^{\ddagger} compare well with those obtained by VT-NMR experiments reported in Tables 3–5. Barriers are nonetheless

Table 5. Computed Dihedral Angles of 1c and 2c,k Calculated at 298 K using IEFPCM/M06/6-31G and IEFPCM/MP2/6-31G**/M06/6-31G****


compd	Φ^a	Θ^b
(P)-1c	117.2	63.7
TS-1c	-154.9	-66.6
(M)-1c	-55.2	61.7
(P)-2c	121.6	65.8
TS-2c	-151.6	37.4
(M)-2c	-55.0	62.2
(P)-2k	131.8	63.7
TS-2k	-143.4	18.5
(M)-2k	-56.9	62.2

^aC2–C3–C6'–C1' dihedral angle in degree. ^bC3–C4–C5–C6 dihedral angle in degree.

slightly higher ($\sim 10 \text{ kJ mol}^{-1}$) than experimental values, due to the fact that accurate transition state energy determination by DFT methods requires meticulous calculations and still remains a challenge.²⁰ A more precise estimation of these energies was achieved by single point calculations using second-order Møller–Plesset perturbation (IEFPCM/MP2/6-31G**/meth-ology).

Also, included in Table 5 are the dihedral angles Φ , featuring the Ar–Csp³ bond rotation limit, and Θ , representing the shape of the monoterpene ring in conformers of 1c and 2c,k. Calculated dihedral angles Φ related to the restricted rotation are found to be similar in both conformers of 1c and 2c,k

likewise for their corresponding TS structures. Indeed, the two rings linked by this bond are almost perpendicular (the aryl ring is slightly oblique) in each conformer, as observed in biaryl systems. Similarly, at the saddle point, the two rings are almost coplanar with Φ in the range of $143\text{--}155^\circ$ in TS-1c and TS-2c,k. Regarding dihedral angles Θ responsible for the conformational changes in the monoterpene ring, the half-chair conformation adopted by each conformer in both alkene and endocyclic epoxide derivatives 1c and 2c,k is confirmed.^{10b} On the other hand, a huge difference was observed in Θ angles in TS-1c versus TS-2c,k. Indeed, a dihedral angle Θ of -66.6° was calculated for the alkene transition state structure (TS-1c), suggesting a ring inversion from diequatorial half-chair form in (P)-1c or (M)-1c to diaxial half-chair form in TS-1c. Therefore, the ΔS^{\ddagger} contribution influenced by this deviation should be positive by favoring more flexible conformational changes, as obtained experimentally in Table 3 for (M)-1c. However, the negative computed value in Table 4 is in contradiction with the experimental value, which is probably due to the difference ($\sim 10 \text{ kJ mol}^{-1}$) found between its $\Delta G^{\ddagger}_{\text{exp}}$ (59.3 kJ mol^{-1}) and $\Delta G^{\ddagger}_{\text{calc}}$ (68.3 kJ mol^{-1}) values. For TS-2c and TS-2k, a calculated dihedral angle Θ of $+37.4^\circ$ and $+18.5^\circ$, respectively, shows that the endocyclic epoxide undergoes a “small” contraction to adopt a diaxial twist chair conformation, meaning that epoxide conformers are less flexible to conformational change. The expected negative ΔS^{\ddagger} value calculated for (P)-2c (Table 4) is in total accordance with the experimental value in Table 3.

Moreover, the MP2 calculated dipole moments for epoxide derivatives 2c,k show significant differences between their conformers versus values found between alkene conformers (P)-1c and (M)-1c (Table 6). This fact implied that it is the

Table 6. Computed Dipole Moments μ of Conformers of 1c and 2c,k at the IEFPCM/MP2/6-31G/M06/6-31G** Level of Theory**

compd	1c		2c		2k	
Epimer	(P)-1c	(M)-1c	(P)-2c	(M)-2c	(P)-2k	(M)-2k
μ (D)	7.40	7.17	9.95	6.63	2.63	3.62

presence of the polar epoxy moiety that intrinsically modifies the polarity of the saturated ring. Interestingly, major conformers (P)-2c and (M)-2k turn out to be the more polar. In these conformers, dipoles resulting from *ortho* substituents on the aryl ring and from the endocyclic epoxide appear to be aligned in a rather more parallel fashion than in the less polar conformers, in which the dipoles are able to oppose one another and would make them more stable. Thus, other stereoelectronic effects associated with or compensating for the polarity of (P)-2c and (M)-2k should make them more stable than the less polar conformers.

To account for this, the second-order perturbation energy $E(2)$ of donor–acceptor interactions in the NBO (natural bond orbital)²¹ basis was calculated for each conformer of 1c and 2c,k at the IEFPCM/M06/6-31G** level of theory, as reported in Figure 5 and Table 7. Indeed, deletion energies obtained by NBO analysis can identify stereoelectronic interactions. In these computed models, the interactions occur mainly between O-substituted groups at the *ortho* positions of the aryl ring and bonds on the C2 (C2=C or C2=O), C3 (C3–H) and C4 (C4–H) carbon atoms in close contact with each other (see O–H, O–C2 interatomic distances in Table S3 in the

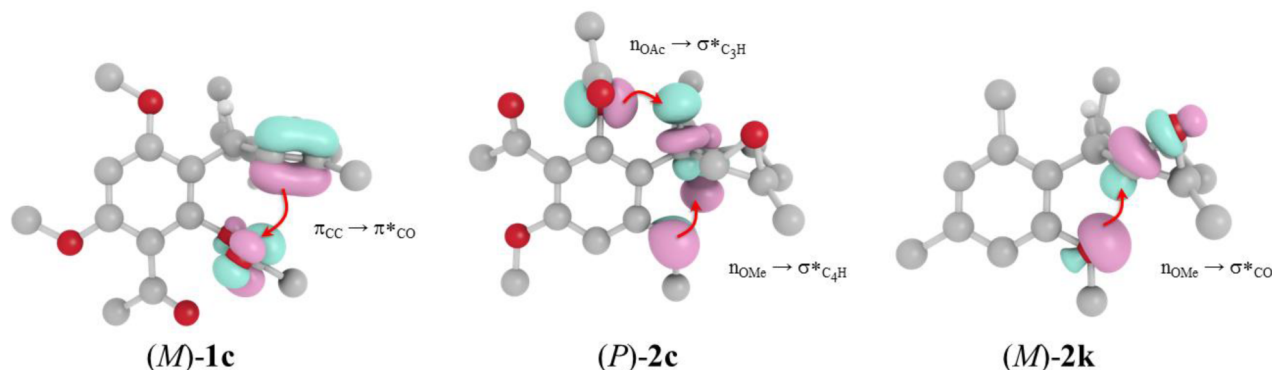


Figure 5. Representative interactions by charge transfer between donor–acceptor in the NBO basis for major conformers (*M*)-**1c**, (*P*)-**2c** and (*M*)-**2k** at the IEFPCM/M06 level of theory.

Table 7. NBO Values of $E(2)$ (kJ mol^{-1}) for **1c** and **2c,k** at the IEFPCM/M06 Level of Theory

compd	$O_{lp} \rightarrow \sigma^*_{C2-O}$		$O_{lp} \rightarrow \sigma^*_{C3-H}$		$O_{lp} \rightarrow \sigma^*_{C4-H}$		$\pi_{C2=C} \rightarrow \pi^*_{C=O}$	total
	OAc	OMe	OAc	OMe	OAc	OMe		
(<i>P</i>)- 1c			1.93, 3.48			3.22		8.62
(<i>M</i>)- 1c				5.36	2.72		4.77	12.85
(<i>P</i>)- 2c		2.68	1.55			1.63, 1.80		7.66
(<i>M</i>)- 2c	2.14			4.86	<1.05			6.99
(<i>P</i>)- 2k				5.28				5.28
(<i>M</i>)- 2k		3.18				1.63, 1.80		5.95

Supporting Information). It is noteworthy that the interactions between O atoms at the *ortho* positions and the C3–H proton observed by ^1H NMR (Figures 2 and 3, Tables S1 and S2 in the Supporting Information) correlate well with these calculations. And in particular, lone pairs of the OMe group lead to the strongest interactions compared to those of the OAc group.²²

In the case of alkene conformers of **1c**, two sets of close intramolecular contacts were highlighted: (1) between oxygen lone pairs at *ortho* positions of OMe and OAc groups (donors) and the σ^* antibonding orbital of C3–H and C4–H bonds (acceptors), (2) between the π bonding orbital of C2=C bond (donor) and the π^* antibonding orbital of the C=O bond of the OAc group (acceptor). The sum of the amounts of the charge transfer between donor and acceptor is in favor of conformer (*M*)-**1c**, making it more stable. Note that $E(2)$ quantities for interactions $O_{lp} \rightarrow \sigma^*_{C3-H}$ and $\pi_{C2=C} \rightarrow \pi^*_{C=O}$ are the highest in this conformer versus (*P*)-**1c**.

In the conformers of epoxide **2c**, $O_{lp} \rightarrow \sigma^*_{C2-O}$ interaction occurs in addition to the interactions between *ortho* oxygen lone pairs and the σ^* antibonding orbital of C3–H and C4–H bonds. (*P*)-**2c** conformer is thereby more stabilized than (*M*)-**2c** by total electron transfers from filled to vacant orbitals (7.66 against 6.99 kJ mol^{-1}). Likewise, for conformers of **2k**, two interactions ($O_{lp} \rightarrow \sigma^*_{C2-O}$ and $O_{lp} \rightarrow \sigma^*_{C4-H}$) occur in favor of (*M*)-**2k** whereas only one ($O_{lp} \rightarrow \sigma^*_{C3-H}$) for (*P*)-**2k**.

These interactions could reasonably be extended to explain the stereoselectivity observed in the rotamers of alkenes **1a,i,k,l** (Figure 3) and in rotamers of epoxides **2i,l** (Figure 2). Indeed, for compounds bearing similar *ortho* substituents, such as the computed models (**1i,k** and **2i**), the formation of major conformers (*M*)-**1i**, (*P*)-**1k** and (*M*)-**2i** could easily be explained by similar charge transfer interactions. Thus, by comparison of **1c** (model) and **1i** conformers, (*M*)-**1i** appears more stabilized than (*P*)-**1i** by two interactions ($\pi_{C2=C} \rightarrow \pi^*_{C=O}$ and $O_{lp} \rightarrow \sigma^*_{C4-H}$) against one for (*P*)-**1i** ($O_{lp} \rightarrow$

σ^*_{C3-H}). In case of **1k**, (*P*)-**1k** is the more stabilized conformer due to $O_{lp} \rightarrow \sigma^*_{C3-H}$ stronger interaction than $O_{lp} \rightarrow \sigma^*_{C4-H}$ interaction in (*M*)-**1k**. In conformers of **2i** compared to those of **2k** (model), two interactions ($O_{lp} \rightarrow \sigma^*_{C2-O}$ and $O_{lp} \rightarrow \sigma^*_{C4-H}$) are in favor of (*M*)-**2i**, whereas only one for (*P*)-**2i** ($O_{lp} \rightarrow \sigma^*_{C3-H}$). For conformers in **1a,l** and **2l**, the poor stereoselectivity could also be explained by the fact that their *ortho*-substituents induce either equivalent interactions (**1a**) or no interaction at all (**1l** and **2l**). However, in the more complicated cases with OPiv group as *ortho*-substituent(s), as in the conformers of **1d,j** (Figure 3) and **2d,j** (Figure 2), it is more difficult to rationalize the formation of the major conformers, which requires a more detailed computational analysis.

CONCLUSION

Some new cannabidiol and linderatin derivatives were synthesized by a terpenylation reaction. Spectroscopic NMR and computational studies of their conformational exchanges were carried out on both alkene and epoxide derivatives to identify clearly the different parameters that influence the restriction to aryl–Csp³ bond rotation. The structures of each conformer in alkenes **1a,c,d,i–l** and epoxides **2c,d,i–l** were determined by means of ^1H NMR and NOESY spectra, and those for **1c** and **2c,k** were also confirmed by DFT computation, which also identified transition structures. VT-NMR spectra provided the barriers and activation parameters for the conformational processes, which were reasonably in line with the computed data. Comparison of the results from differently substituted compounds highlighted unusual stereoelectronic effects influencing the formation of the major and the minor conformers.

From these results, we have demonstrated that the potential for atropisomerism with high diastereoselectivity in these natural product derivatives depends mainly on the nature of the two *ortho* substituents in association with the epoxy moiety.

The combination of a substituted oxygen and a hindered methyl group at *ortho* positions in epoxide **2i–k** conformers can exhibit atropisomerism.

EXPERIMENTAL SECTION

1-(2,4-Dihydroxy-3-((1*R*,6*R*)-6-isopropyl-3-methylcyclohex-2-enyl)phenyl)ethanone (1e). A solution of 2',6'-dihydroxyacetophenone (152 mg, 1 mmol) in dry CH₃CN (5 mL) was added dropwise to a suspension of (–)- α -phellandrene (0.4 mL, 2.5 mmol) and TsOH (273 mg, 1.5 mmol) in dry toluene (10 mL) at 0 °C under a N₂ atmosphere. The mixture was stirred for 3 h at 0 °C. After neutralization with saturated NaHCO₃, the mixture was extracted with EtOAc. The combined extracts were washed, dried, and evaporated. The residue was chromatographed (3:7 CH₂Cl₂/petroleum ether) to give **1e** (128 mg, 44%) as a crystalline yellow solid: mp 94–96 °C; [α]_D²¹ + 80.7 (c 1.9, CHCl₃); ¹H NMR (300 MHz, CDCl₃) δ 10.73 (br s, 1H), 9.08 (br s, 1H), 7.09 (d, *J* = 8.4 Hz, 1H), 6.38 (d, *J* = 8.4 Hz, 1H), 5.40 (s, 1H), 3.39 (br dt, *J* = 9.1 Hz, *J* = 2.4 Hz, 1H), 2.74 (s, 3H), 2.10 (m, 2H), 1.80 (s, 3H), 1.79–1.30 (m, 4H), 0.89 (d, *J* = 6.8 Hz, 3H), 0.82 (d, *J* = 6.8 Hz, 3H); ¹³C NMR (75 MHz, CDCl₃) δ 205.6 (C), 160.6 (C), 158.9 (C), 139.0 (C), 137.3 (CH), 124.1 (CH), 121.9 (C), 110.7 (C), 107.7 (CH), 44.3 (CH), 41.4 (CH), 33.7 (CH₃), 30.3 (CH₂), 27.3 (CH), 23.7 (CH₃), 21.6 (CH₂), 21.57 (CH₃), 16.4 (CH₃); IR (NaCl) 3333, 2951, 2925, 1620, 1597, 1429, 1370, 1241, 1225, 1042, 807, 758 cm⁻¹; MS (EI) *m/z* (rel intensity, %) 288 (M⁺, 44), 245 (23), 218 (58), 203 (100), 165 (34), 149 (70); HRMS (EI-TOF) *m/z* calcd for C₁₈H₂₄O₃ 288.1725, found 288.1734. Anal. Calcd for C₁₈H₂₄O₃: C, 74.97; H, 8.39. Found: C, 75.22; H, 8.59.

2-((1*R*,6*R*)-6-isopropyl-3-methylcyclohex-2-enyl)-3,5-dimethylbenzene-1-ol (1h). A solution of 3,5-dimethylphenol (934 mg, 7.6 mmol) in dry toluene (10 mL) was added dropwise to a suspension of (–)- α -phellandrene (3 mL, 18.6 mmol) and TsOH (2.21 g, 11.6 mmol) in dry toluene (70 mL) at rt under a N₂ atmosphere. The mixture was stirred for 3 h at rt. After neutralization with saturated NaHCO₃, the mixture was extracted with EtOAc. The combined extracts were washed, dried, and evaporated. The residue was chromatographed (98:2 petroleum ether/EtOAc) to give **1h** (1.06 g, 54%) as a liquid: [α]_D²⁴ + 83.6 (c 1.8, CHCl₃); ¹H NMR (300 MHz, CDCl₃) δ 6.56 (s, 1H), 6.54 (s, 1H), 5.94 (s, 1H), 5.49 (s, 1H), 3.52 (br d, *J* = 9.2 Hz, 1H), 2.27 (s, 3H), 2.24 (s, 3H), 2.21–2.01 (m, 2H), 1.88–1.65 (m, 4H), 1.63–1.48 (m, 2H), 1.45–1.20 (m, 1H), 0.88 (m, 6H); ¹³C NMR (75 MHz, CDCl₃) δ 155.4 (C), 139.7 (C), 137.6 (C), 137.0 (C), 125.3 (C), 124.8 (CH), 123.4 (CH), 116.0 (CH), 42.9 (CH), 39.0 (CH), 30.6 (CH₂), 27.4 (CH), 23.6 (CH₃), 22.1 (CH₂), 21.9 (CH₃), 20.8 (2 CH₃), 16.7 (CH₃); IR (NaCl) 3447, 2951, 2925, 2357, 1620, 1571, 1455, 1305, 1282, 1042, 838 cm⁻¹; MS (EI) *m/z* (rel intensity, %) 258 (M⁺, 41), 188 (36), 173 (100), 135 (28); HRMS (EI-TOF) *m/z* calcd for C₁₈H₂₆O 258.1984, found 258.1982. Anal. Calcd for C₁₈H₂₆O: C, 83.67; H, 10.14. Found: C, 83.48; H, 10.08.

General Procedure for the Synthesis of Pivalates 1d,g,j. PivCl (1 mL) was added to a solution of **1a**, **1e** or **1h** (0.3 mmol) in pyridine (1 mL) at rt under a N₂ atmosphere, and the mixture was stirred at 80 °C overnight. The reaction mixture was evaporated under reduced pressure, and the residue was purified by silica gel column chromatography to give pivalates **1d**, **1g** or **1j**.

2-Acetyl-4-((1*R*,6*R*)-6-isopropyl-3-methylcyclohex-2-enyl)-benzene-1,3,5-triyl tris(2,2-dimethylpropanoate) (1d). 79%, liquid: [α]_D²⁴ + 45.96 (c 2.08, CHCl₃); ¹H NMR (300 MHz, CDCl₃) δ 6.71 (s, 1H), 5.67 (s, 1H), 3.44 (br s, 1H), 2.42 (s, 3H), 2.12–1.63 (m, 5H), 1.58 (s, 3H), 1.50–1.16 (m, 28H), 0.81 (d, *J* = 6.9 Hz, 3H), 0.72 (d, *J* = 6.9 Hz, 3H); ¹³C NMR (75 MHz, CDCl₃) δ 198.9 (C), 176.3 (2 C), 175.8 (C), 151.2 (C), 146.9 (C), 145.5 (C), 132.9 (C), 128.3 (C), 126.5 (C), 124.5 (CH), 115.3 (CH), 42.2 (CH), 39.2 (C), 39.1 (C), 39.0 (C), 38.1 (CH), 31.6 (CH₃), 31.0 (CH₂), 27.9 (CH), 27.1 (6 CH₃), 27.0 (3 CH₃), 23.2 (CH₃), 22.9 (CH₂), 21.5 (CH₃), 15.9 (CH₃); IR (NaCl) 2961, 2930, 1760, 1708, 1602, 1478, 1269, 1093, 1037, 755 cm⁻¹; MS (EI) *m/z* (rel intensity,

%) 556 (M⁺, 7), 471 (31), 387 (100), 303 (15); HRMS (EI-TOF) *m/z* calcd for C₃₃H₄₈O₇ 556.3400, found 556.3387.

2-Acetyl-4-((1*R*,6*R*)-6-isopropyl-3-methylcyclohex-2-enyl)-1,3-phenylene bis(2,2-dimethylpropanoate) (1g). 60%, liquid: [α]_D²¹ + 76.9 (c 1.5, CHCl₃); ¹H NMR (300 MHz, CDCl₃) δ 7.27 (d, *J* = 8.7 Hz, 1H), 6.88 (d, *J* = 8.7 Hz, 1H), 5.11 (s, 1H), 3.30 (br m, 1H), 2.42 (s, 3H), 2.20–1.94 (m, 2H), 1.84–1.43 (m, 7H), 1.41–1.24 (m, 18H), 0.82 (d, *J* = 6.8 Hz, 3H), 0.74 (d, *J* = 6.8 Hz, 3H); ¹³C NMR (75 MHz, CDCl₃) δ 199.5 (C), 176.5 (C), 176.2 (C), 145.5 (C), 145.3 (C), 136.5 (C), 134.3 (C), 130.2 (CH), 128.3 (C), 124.8 (CH), 120.1 (CH), 45.7 (CH), 39.2 (CH), 39.1 (C), 39.0 (C), 31.6 (CH₃), 30.6 (CH₂), 27.4 (CH), 27.1 (3CH₃), 27.0 (3CH₃), 23.5 (CH₃), 22.0 (CH₂), 21.6 (CH₃), 16.3 (CH₃); MS (EI) *m/z* (rel intensity, %) 456 (M⁺, 1.5), 371 (91), 287 (100), 203 (31), 165 (27), 85 (40); HRMS (EI-TOF) *m/z* calcd for C₂₈H₄₀O₅ 456.2876, found 456.2873.

2-((1*R*,6*R*)-6-isopropyl-3-methylcyclohex-2-enyl)-3,5-dimethylphenyl pivalate (1j). 56%, liquid: [α]_D²⁴ + 69.1 (c 0.44, CHCl₃); ¹H NMR (300 MHz, CDCl₃) δ 6.82 (s, 1H), 6.51 (br s, 1H), 5.21 (br s, 1H), 3.52 (br s, 1H), 2.32 (s, 3H), 2.26 (s, 3H), 2.12–1.72 (m, 4H), 1.62 (br s, 3H), 1.48–1.08 (m, 11H), 0.81 (d, *J* = 6.8 Hz, 3H), 0.77 (d, *J* = 6.8 Hz, 3H); ¹³C NMR (75 MHz, CDCl₃) δ 174.1 (C), 150.5 (C), 138.5 (C), 136.3 (C), 132.1 (C), 130.8 and 128.7 (CH), 126.1 and 125.1 (CH), 122.0 and 120.1 (CH), 42.5 (CH), 122.4 (CH), 40.3 (CH), 40.1 (C), 29.8 (CH₂), 27.9 (CH), 27.4 (CH₃), 27.1 (CH₃), 26.6 (CH₃), 23.4 (CH₃), 23.1 (CH₂), 21.9 (CH₃), 20.8 (2 CH₃), 16.7 (CH₃); IR (NaCl) 2956, 2925, 1749, 1476, 1458, 1269, 1117, 1034, 845, 758 cm⁻¹; MS (EI) *m/z* (rel intensity, %) 342 (M⁺, 34), 257 (57), 241 (31), 173 (100), 171 (67), 135 (31); HRMS (EI-TOF) *m/z* calcd for C₂₃H₃₄O₂ 342.2559, found 342.2555.

General Procedure for the Synthesis of Acetates 1fi. Ac₂O (1.5 mL) was added to a solution of **1e** or **1h** (0.25 mmol) in pyridine (1 mL) at rt under a N₂ atmosphere, and the whole was stirred at rt for 3h (for **1i**) or 80 °C overnight (for **1f**). The reaction mixture was evaporated under reduced pressure, and then the residue was purified by silica gel column chromatography to give acetates **1f** or **1i**.

2-Acetyl-4-((1*R*,6*R*)-6-isopropyl-3-methylcyclohex-2-enyl)-1,3-phenylene diacetate (1f). 92%, liquid: [α]_D²¹ + 70.8 (c 1.3, CHCl₃); ¹H NMR (300 MHz, CDCl₃) δ 7.30 (d, *J* = 8.6 Hz, 1H), 7.03 (d, *J* = 8.6 Hz, 1H), 5.14 (d, *J* = 1.0 Hz, 1H), 3.38 (br m, 1H), 2.45 (s, 3H), 2.29 (s, 3H), 2.24 (s, 3H), 2.03 (m, 2H), 1.79–1.65 (m, 4H), 1.58–1.32 (m, 3H), 0.87 (d, *J* = 6.7 Hz, 3H), 0.79 (d, *J* = 6.7 Hz, 3H); ¹³C NMR (75 MHz, CDCl₃) δ 199.4 (C), 169.1 (C), 168.6 (C), 145.6 (C), 145.4 (C), 136.7 (C), 135.3 (CH), 131.4 (CH), 127.6 (C), 123.8 (CH), 120.3 (CH), 45.8 (CH), 39.3 (CH), 31.0 (CH₃), 29.8 (CH₂), 27.3 (CH), 23.4 (CH₃), 21.6 (CH₃), 21.3 (CH₂), 21.1 (CH₃), 20.8 (CH₃), 16.9 (CH₃); IR (NaCl) 2956, 2925, 1770, 1700, 1470, 1367, 1186, 1037 cm⁻¹; MS (EI) *m/z* (rel intensity, %) 372 (M⁺, 0.7), 329 (71), 287 (100), 218 (85), 203 (73), 165 (48); HRMS (EI-TOF) *m/z* calcd for C₂₂H₂₈O₅ 372.1937, found 372.1953. Anal. Calcd for C₂₂H₂₈O₅: C, 70.94; H, 7.58. Found: C, 70.77; H, 7.65.

2-((1*R*,6*R*)-6-isopropyl-3-methylcyclohex-2-enyl)-3,5-dimethylphenyl acetate (1i). 80%, liquid: [α]_D²⁴ + 138.3 (c 0.4, CHCl₃); ¹H NMR (300 MHz, CDCl₃) δ 6.84 (br s, 1H), 6.62 (br s, 1H), 5.16 (br s, 1H), 3.50 (br s, 1H), 2.31 (s, 3H), 2.27 (s, 3H), 2.21–1.91 (m, 5H), 1.78 (dt, *J* = 12.7 Hz, *J* = 2.3 Hz, 1H), 1.66 (s, 3H), 1.51–1.21 (m, 3H), 0.82 (m, 6H); ¹³C NMR (75 MHz, CDCl₃) δ 169.9 (C), 149.5 (C), 138.6 (C), 136.2 (C), 132.6 (C), 131.9 (C), 128.9 (CH), 125.6 (CH), 122.4 (CH), 42.7 (CH), 39.8 (CH), 30.7 (CH₂), 27.7 (CH), 23.4 (CH₃), 22.5 (CH₂), 21.8 (CH₃), 21.0 (CH₃), 20.7 (2 CH₃), 16.8 (CH₃); IR (NaCl) 2951, 2920, 1762, 1445, 1362, 1259, 1204, 1127, 1042, 869, 796 cm⁻¹; MS (EI) *m/z* (rel intensity, %) 300 (M⁺, 38), 258 (24), 215 (23), 188 (47), 173 (100), 170 (46), 135 (30); HRMS (EI-TOF) *m/z* calcd for C₂₀H₂₈O₂ 300.2089, found 300.2100.

2-((1*R*,6*R*)-6-isopropyl-3-methylcyclohex-2-enyl)-1-methoxy-3,5-dimethylbenzene (1k). A suspension of phenol **1h** (110 mg, 0.43 mmol), Me₂SO₄ (0.1 mL, 110 mg, 0.9 mmol), and anhydrous K₂CO₃ (147 mg, 1.08 mmol) in Me₂CO (6 mL) was stirred under reflux for 4 h. The reaction was filtered and evaporated under reduced

pressure to give a residue that was purified by column chromatography (petroleum ether) to yield **1k** (90 mg, 77%) as a liquid: $^1\text{H NMR}$ (300 MHz, CDCl_3) δ 6.56 (s, 1H), 6.54 (s, 1H), 5.20 (br s, 1H), 4.14 (br s, 0.75H), 3.74 (br s, 3H), 3.43 (br s, 0.25H), 2.28 (br s, 6H), 2.15–1.95 (m, 2H), 1.90–1.70 (m, 2H), 1.66 (br s, 3H), 1.50–1.30 (m, 2H), 0.80 (d, $J = 6.9$ Hz, 3H), 0.79 (d, $J = 6.9$ Hz, 3H); $^{13}\text{C NMR}$ (75 MHz, CDCl_3) δ 138.3 (C), 135.9 (C), 132.8 (C), 128.6 (C), 126.4 (CH), 125.1 (CH), 109.0 (CH), 55.7 (CH₃), 42.8 (CH), 36.3 (CH), 30.9 (CH₂), 28.0 (CH), 23.3 (CH₃), 22.9 (CH₂), 21.8 (CH₃), 21.2 (CH₃), 20.1 (CH₃), 16.0 (CH₃); MS (EI) m/z (rel intensity, %) 272 (M^+ , 32), 202 (56), 187 (100), 171 (26), 149 (14); HRMS (EI-TOF) m/z calcd for $\text{C}_{19}\text{H}_{28}\text{O}$ 272.2140, found 272.2147.

(M,P)-2-((1R,6R)-6-isopropyl-3-methylcyclohex-2-enyl)-1-ethyl-3,5-dimethylbenzene (1l). To the phenol **1h** (219 mg, 0.85 mmol) in anhydrous CH_2Cl_2 (5 mL) was added pyridine (0.14 mL, 0.13 mmol, 1.7 mmol) and the solution was cooled to 0 °C. Ti_2O (0.15 mL, 263 mg, 1.1 mmol) was added dropwise and the mixture was warmed to rt. The reaction was complete within 5 min as shown by TLC. The mixture was diluted with CH_2Cl_2 (5 mL), quenched with 10% aq HCl and washed successively with sat NaHCO_3 and brine. After drying on MgSO_4 the solvent was evaporated and the residue was purified by column chromatography on silica gel (petroleum ether) to give the triflate (279 mg, 85%) as a liquid.^{25a}

To a solution of the triflate (279 mg, 0.72 mmol) in dry THF (5 mL) were added a 5% Pd(PPh_3)₄ (40 mg, 0.04 mmol) and Et_3Al (0.2 mL, 163 mg, 1.44 mmol). The mixture was refluxed under argon atmosphere for 2 days. The reaction was followed by TLC. The reaction solution was evaporated to dryness, CH_2Cl_2 (10 mL) was added, and the residue was washed with brine. Chromatography on silica gel (petroleum ether) yielded **1l** (45 mg, 23%) as a liquid.^{25b} dr 45/55; $^1\text{H NMR}$ (400 MHz, CDCl_3) δ 6.78 (s, 0.45H), 6.74 (s, 0.55H), 6.73 (s, 0.45H), 6.71 (s, 0.55H), 5.21 (s, 0.45H), 5.16 (s, 0.55H), 3.57 (br d, $J = 10.2$ Hz, 1H), 2.82 (dq, $J = 14.3$ Hz, $J = 7.4$ Hz, 0.55H), 2.74 (q, $J = 7.5$ Hz, 0.9H), 2.49 (dq, $J = 14.3$ Hz, $J = 7.4$ Hz, 0.55H), 2.23 (s, 3H), 2.18 (s, 3H), 2.10–1.65 (m, 4H), 1.59 (s, 3H), 1.42–1.22 (m, 2H), 1.07 (m, 3H), 0.8–0.7 (m, 6H); $^{13}\text{C NMR}$ (75 MHz, CDCl_3) δ 143.9 (C), 143.7 (C), 138.0 (C), 137.6 (C), 137.3 (C), 135.1 (C), 133.5 (C), 132.5 (C), 131.2 (CH), 129.5 (CH), 128.7 (CH), 127.4 (CH), 126.6 (CH), 126.0 (CH), 44.2 (CH), 42.3 (CH), 41.0 (CH), 40.6 (CH), 30.8 (CH₂), 30.7 (CH₂), 27.9 (CH₂), 27.5 (CH), 27.4 (CH), 25.2 (CH₂), 23.4 (CH₃), 23.3 (CH₃), 22.9 (CH₂), 22.8 (CH₂), 22.1 (CH₃), 22.06 (CH₃), 20.8 (CH₃), 16.8 (CH₃), 16.3 (CH₃); MS (EI) m/z (rel intensity, %) 270 (M^+ , 22), 185 (52), 171 (100), 157 (27); HRMS (EI-TOF) m/z calcd for $\text{C}_{20}\text{H}_{30}$ 270.2348, found 270.2348.

General Procedure for the Synthesis of Epoxides 2d,f,g,i-l. *m*-CPBA (1.2 equiv) was added to a solution of **1d,f,g,i-l** in CH_2Cl_2 at rt under a N_2 atmosphere, and the whole was stirred for 0.5–1 h. The reaction mixture was treated with saturated NaHCO_3 and extracted with CH_2Cl_2 . The organic layer was dried and evaporated. The residue was purified by silica gel column chromatography to give either rotameric, atropisomeric or single epoxide(s).

(P,M)-2-Acetyl-4-((1S,2S,3R,6R)-3-isopropyl-6-methyl-7-oxabicyclo[4.1.0]heptan-2-yl)benzene-1,3,5-triyl tris(2,2-dimethylpropanoate) (2d). 90%, amorphous solid: dr 68/32; $^1\text{H NMR}$ (300 MHz, CDCl_3) δ 6.84 (s, 0.32H), 6.73 (s, 0.68H), 3.13 (d, $J = 12.2$ Hz, 0.32H), 2.98 (d, $J = 12.1$ Hz, 0.68H), 2.95 (s, 0.32H), 2.90 (s, 0.68H), 2.44 (s, 2.04H), 2.43 (s, 0.96H), 2.19 (m, 2H), 1.82–0.82 (m, 34H), 0.76 (d, $J = 6.9$ Hz, 2.04H), 0.75 (d, $J = 6.9$ Hz, 0.96H), 0.66 (d, $J = 6.9$ Hz, 2.04H), 0.65 (d, $J = 6.9$ Hz, 0.96H); $^{13}\text{C NMR}$ (75 MHz, CDCl_3) δ 199.1 (C), 198.5 (C), 176.8 (C), 176.6 (C), 176.4 (C), 176.2 (C), 175.8 (C), 151.3 (C), 151.1 (C), 147.1 (C), 146.4 (C), 146.2 (C), 126.5 (C), 126.3 (C), 126.2 (C), 115.6 (CH), 114.9 (CH), 64.3 (CH), 64.1 (CH), 58.2 (C), 41.5 (CH), 41.3 (CH), 39.5 (C), 39.4 (C), 39.3 (C), 39.2 (C), 39.18 (C), 39.0 (CH), 38.8 (CH), 31.8 (CH₃), 31.6 (CH₃), 30.8 (CH₂), 29.8 (CH₂), 28.1 (CH), 27.9 (CH), 27.4–27.1 (CH₃, *t*-Bu), 23.1 (CH₃), 21.4 (CH₃), 21.2 (CH₃), 19.24 (CH₂), 19.2 (CH₂), 15.6 (CH₃), 15.5 (CH₃); IR (NaCl) 2961, 1760, 1708, 1478, 1266, 1088, 1039, 755 cm^{-1} ; MS (EI) m/z (rel intensity, %) 572 (M^+ , 0.5), 470 (18), 385 (100), 316 (58), 301 (59), 259 (46),

85 (42); HRMS (EI-TOF) m/z calcd for $\text{C}_{33}\text{H}_{48}\text{O}_8$ 572.3349, found 572.3356.

2-Acetyl-4-((1S,2S,3R,6R)-3-isopropyl-6-methyl-7-oxabicyclo[4.1.0]heptan-2-yl)-1,3-phenylene diacetate (2f). 72%, crystalline solid: mp 105–107 °C; $[\alpha]_{\text{D}}^{21} + 34.9$ (c 0.75, CHCl_3); $^1\text{H NMR}$ (300 MHz, CDCl_3) δ 7.29 (d, $J = 8.6$ Hz, 1H), 7.10 (d, $J = 8.6$ Hz, 1H), 3.04 (br d, $J = 9.6$ Hz, 1H), 2.81 (br s, 1H), 2.47 (s, 3H), 2.30 (s, 3H), 2.29 (s, 3H), 2.12 (m, 1H), 1.82–1.58 (m, 2H), 1.46–1.17 (m, 6H), 0.78 (d, $J = 6.8$ Hz, 3H), 0.72 (d, $J = 6.8$ Hz, 3H); $^{13}\text{C NMR}$ (75 MHz, CDCl_3) δ 199.1 (C), 168.9 (C), 168.5 (C), 146.1 (C), 145.5 (C), 134.5 (C), 131.1 (CH), 128.1 (C), 120.8 (CH), 63.6 (CH), 58.3 (C), 40.4 (CH), 38.8 (CH), 31.1 (CH₃), 30.8 (CH₂), 26.8 (CH), 23.4 (CH₃), 21.3 (CH₃), 21.1 (CH₃), 20.9 (CH₃), 17.5 (CH₂), 15.8 (CH₃); IR (KBr) 3426, 2956, 2941, 1770, 1698, 1370, 1210, 1184, 1037 cm^{-1} ; MS (EI) m/z (rel intensity, %) 388 (M^+ , 0.5), 346 (21), 286 (74), 243 (100), 216 (73), 203 (36), 165 (85); HRMS (EI-TOF) m/z calcd for $\text{C}_{22}\text{H}_{28}\text{O}_6$ 388.1886, found 388.1888. Anal. Calcd for $\text{C}_{22}\text{H}_{28}\text{O}_6$: C, 68.02; H, 7.27. Found: C, 67.95; H, 7.35.

2-Acetyl-4-((1S,2S,3R,6R)-3-isopropyl-6-methyl-7-oxabicyclo[4.1.0]heptan-2-yl)-1,3-phenylene bis(2,2-dimethylpropanoate) (2g). 68%, amorphous solid: $[\alpha]_{\text{D}}^{24} + 54.8$ (c 0.95, CHCl_3); $^1\text{H NMR}$ (300 MHz, CDCl_3) δ 7.31 (d, $J = 8.5$ Hz, 1H), 7.06 (d, $J = 8.5$ Hz, 1H), 2.99 (br d, $J = 10.9$ Hz, 1H), 2.74 (br s, 1H), 2.44 (s, 3H), 2.11 (m, 1H), 1.82–1.65 (m, 2H), 1.50–1.16 (m, 24H), 0.78 (d, $J = 6.8$ Hz, 3H), 0.68 (d, $J = 6.8$ Hz, 3H); $^{13}\text{C NMR}$ (75 MHz, CDCl_3) δ 199.1 (C), 176.5 (C), 176.2 (C), 146.0 (C), 145.6 (C), 134.2 (C), 129.1 (CH), 128.9 (C), 120.5 (CH), 63.7 (CH), 58.1 (C), 44.7 (CH), 39.8 (CH), 39.1 (C), 37.9 (CH), 31.5 (CH₃), 30.8 (CH₂), 27.9 (CH₃), 27.1 (CH₃), 27.1 (CH₃), 27.0 (CH₃), 26.7 (CH₃), 22.9 (CH₃), 21.3 (CH₃), 17.8 (CH₂), 16.1 (CH₃); IR (NaCl) 2956, 1755, 1706, 1473, 1223, 1096 cm^{-1} ; MS (EI) m/z (rel intensity, %) 472 (M^+ , 4), 285 (36), 243 (38), 216 (44), 165 (20), 57 (100); HRMS (EI-TOF) m/z calcd for $\text{C}_{28}\text{H}_{40}\text{O}_6$ 472.2825, found 472.2820.

(M,P)-2-((1S,2S,3R,6R)-3-Isopropyl-6-methyl-7-oxabicyclo[4.1.0]heptan-2-yl)-3,5-dimethylphenyl acetate (2i). 90%, amorphous solid: dr 59/41; R_f in 8% EtOAc/hexane = 0.27 and 0.24, HPLC (Silica, 10% EtOAc/hexane) retention times of the epimers (*M*) 5.7 min and (*P*) 6.1 min dr 67/33; $^1\text{H NMR}$ (300 MHz, CDCl_3) δ 6.88 (s, 1H), 6.71 (s, 0.59H), 6.69 (s, 0.41H), 3.25 (d, $J = 11.0$ Hz, 0.41H), 3.11 (d, $J = 11.2$ Hz, 0.59H), 2.89 (s, 0.41H), 2.86 (s, 0.59H), 2.40–2.25 (m, 9H), 2.21–2.03 (m, 1H), 1.89–1.59 (m, 1H), 1.51–1.13 (m, 6H), 1.00–0.70 (m, 7H); $^{13}\text{C NMR}$ (75 MHz, CDCl_3) δ 169.5 (C), 169.4 (C), 149.4 (C), 149.2 (C), 138.7 (C), 137.0 (C), 136.9 (C), 130.6 (C), 130.5 (CH), 130.2 (C), 128.8 (CH), 121.8 (CH), 120.3 (CH), 64.5 (CH), 64.0 (CH), 58.7 (C), 58.4 (C), 43.1 (CH), 42.6 (CH), 39.1 (CH), 36.7 (CH), 30.9 (CH₂), 30.2 (CH₂), 27.6 (CH), 27.5 (CH), 23.1 (CH₃), 22.5 (CH₃), 21.6 (CH₃), 21.5 (CH₃), 21.1 (CH₃), 21.0 (CH₃), 20.8 (CH₃), 20.7 (CH₃), 18.1 (CH₂), 17.7 (CH₂), 16.5 (CH₃), 15.9 (CH₃); IR (NaCl) 2951, 1765, 1450, 1365, 1204, 1039, 869 cm^{-1} ; MS (EI) m/z (rel intensity, %) 316 (M^+ , 19), 256 (27), 231 (59), 213 (100), 186 (37), 173 (56), 135 (70); HRMS (EI-TOF) m/z calcd for $\text{C}_{20}\text{H}_{28}\text{O}_3$ 316.2038, found 316.2037. Anal. Calcd for $\text{C}_{20}\text{H}_{28}\text{O}_3$: C, 75.91; H, 8.92. Found: C, 75.94; H, 8.97.

(M,P)-2-((1S,2S,3R,6R)-3-Isopropyl-6-methyl-7-oxabicyclo[4.1.0]heptan-2-yl)-3,5-dimethylphenyl pivalate (2j). 70%, amorphous solid: dr 30/70; R_f in 10% EtOAc/hexane = 0.33 and 0.27, HPLC (Silica, 10% EtOAc/hexane) retention times of the epimers (*M*) 3.8 min and (*P*) 4.2 min dr 27/73; $^1\text{H NMR}$ (300 MHz, CDCl_3) δ 6.86 (s, 1H), 6.60 (s, 0.7H), 6.49 (s, 0.3H), 3.19 (d, $J = 11.4$ Hz, 0.7H), 3.11 (d, $J = 11.9$ Hz, 0.3H), 2.91 (s, 1H), 2.49 (s, 0.9H), 2.47 (s, 2.1H), 2.28 (s, 2.1H), 2.27 (s, 0.9H), 2.10 (m, 1H), 1.88–1.10 (m, 16H), 1.01–0.63 (m, 7H); $^{13}\text{C NMR}$ (75 MHz, CDCl_3) δ 177.5 (C), 177.3 (C), 150.6 (C), 150.0 (C), 138.9 (C), 137.0 (C), 136.9 (C), 130.5 (C), 130.3 (CH), 128.8 (CH), 121.3 (CH), 120.1 (CH), 64.9 (CH), 64.1 (CH), 58.6 (C), 58.3 (C), 42.3 (CH), 41.9 (CH), 40.7 (CH), 39.1 (C), 37.0 (CH), 30.7 (CH₂), 30.3 (CH₂), 27.8 (CH₃), 27.7 (CH₃), 27.3 (CH₃), 26.5 (CH₃), 23.2 (CH₃), 22.5 (CH₃), 21.6 (CH₃), 21.2 (CH), 20.7 (CH₃), 20.4 (CH₃), 19.0 (CH₂), 18.2 (CH₂), 16.3 (CH₃), 16.2 (CH₃); IR (KBr) 3442, 2951, 2925, 2367, 2341, 1698, 1633, 1447, 1310, 1295, 1259, 1111, 1039, 827, 677 cm^{-1} ; MS

(EI) m/z (rel intensity, %) 358 (M^+ , 35), 256 (22), 231 (42), 213 (100), 186 (41), 173 (36), 135 (58); HRMS (EI-TOF) m/z calcd for $C_{23}H_{34}O_3$ 358.2508, found 358.2516.

(M,P)-(1R,4R,5S,6S)-4-Isopropyl-1-methyl-5-(2-methoxy-4,6-dimethylphenyl)-oxabicyclo[4.1.0]heptane (2k). 74%, liquid; dr 78/22; R_f in 5% EtOAc/petroleum ether = 0.27 and 0.23; 1H NMR (300 MHz, $CDCl_3$) δ 6.61 (s, 1H), 6.56 (s, 0.78H), 6.54 (s, 0.22H), 3.81 (d, $J = 10.9$ Hz, 0.22H), 3.78 (s, 2.34H), 3.76 (s, 0.66H), 3.07 (d, $J = 10.6$ Hz, 0.78H), 2.89 (s, 0.22H), 2.81 (s, 0.78H), 2.31 (s, 1.32H), 2.30 (s, 4.68H), 2.04 (dt, $J = 14.2$ Hz, $J = 3.2$ Hz, 1H), 1.85–1.55 (m, 2H), 1.36 (s, 0.66H), 1.34 (s, 2.34H), 1.35–1.25 (m, 3H), 0.81 (d, $J = 6.9$ Hz, 2.34H), 0.79 (d, $J = 6.7$ Hz, 0.66H), 0.74 (d, $J = 6.9$ Hz, 3H); ^{13}C NMR (75 MHz, $CDCl_3$) δ 157.9 (C), 157.7 (C), 137.9 (C), 136.7 (C), 136.6 (C), 127.8 (C), 127.5 (C), 124.7 (CH), 123.5 (CH), 110.0 (CH), 108.9 (CH), 65.7 (CH), 65.1 (CH), 59.0 (C), 58.7 (C), 55.5 (CH₃), 55.1 (CH₃), 43.2 (CH), 42.4 (CH), 38.5 (CH), 34.8 (CH), 30.5 (CH₂), 27.8 (CH), 23.1 (CH₃), 22.7 (CH₃), 21.7 (CH₃), 21.66 (CH₃), 21.3 (CH₃), 20.8 (CH₃), 18.0 (CH₂), 17.8 (CH₂), 16.5 (CH₃), 15.9 (CH₃); MS (EI) m/z (rel intensity, %) 288 (M^+ , 48), 270 (20), 227 (33), 149 (100), 136 (56), 119 (32); HRMS (EI-TOF) m/z calcd for $C_{19}H_{28}O_2$ 288.2089, found 288.2102.

(M,P)-(1R,4R,5S,6S)-4-Isopropyl-1-methyl-5-(2-ethyl-4,6-dimethylphenyl)-oxabicyclo[4.1.0]heptane (2l). 82%, liquid; dr 44/56; 1H NMR (300 MHz, $CDCl_3$) δ 6.91 (s, 0.44H), 6.85 (s, 1H), 6.83 (s, 0.56H), 3.26 (d, $J = 11.1$ Hz, 1H), 2.90 (s, 1H), 2.83 (dq, $J = 14.3$ Hz, $J = 7.4$ Hz, 0.56H), 2.65 (q, $J = 7.5$ Hz, 0.88H), 2.52 (dq, $J = 14.3$ Hz, $J = 7.4$ Hz, 0.56H), 2.35 (s, 1.68H), 2.34 (s, 1.32H), 2.27 (s, 3H), 2.11 (m, 1H), 1.82 (m, 1H), 1.63–1.15 (m, 10H), 0.81 (d, $J = 6.8$ Hz, 1.32H), 0.80 (d, $J = 6.8$ Hz, 1.32H), 0.74 (d, $J = 6.5$ Hz, 1.68H), 0.73 (d, $J = 6.9$ Hz, 1.68H); ^{13}C NMR (75 MHz, $CDCl_3$) δ 143.9 (C), 142.3 (C), 137.4 (C), 136.8 (C), 136.4 (C), 135.9 (C), 135.75 (C), 135.7 (C), 130.9 (CH), 129.0 (CH), 128.8 (CH), 127.5 (CH), 64.83 (CH), 64.8 (CH), 58.9 (C), 58.91 (C), 44.5 (CH), 42.5 (CH), 39.8 (CH), 39.2 (CH), 30.2 (CH₂), 30.16 (CH₂), 27.7 (CH₂), 27.4 (CH), 27.2 (CH), 25.4 (CH₂), 22.7 (CH₃), 22.6 (CH₃), 21.9 (CH₃), 20.8 (CH₃), 18.1 (CH₂), 18.08 (CH₂), 16.9 (CH₃), 16.6 (CH₃), 16.3 (CH₃); MS (EI) m/z (rel intensity, %) 286 (M^+ , 29), 268 (11), 243 (100), 225 (24), 197 (25), 147 (79), 133 (44); HRMS (EI-TOF) m/z calcd for $C_{20}H_{30}O$ 286.2297, found 286.2311.

■ ASSOCIATED CONTENT

■ Supporting Information

1H and ^{13}C NMR spectra of compounds **1d–l** and **2d,f,g,i–l**; 1H NMR spectra at low temperature of **1c,d,i–k**; NOESY spectra of **1a,i–l** and **2c,d,i–l**; VT-HSQC spectra of **1d**; VT 1H NMR spectra of **1a–d,i–l** and **2c,d,f,g,i–l**; line-shape simulated spectra of **1c**; Eyring plots data of **1c** and **2c,j**. HPLC chromatograms of **2i,j**, computational data of **1c** and **2c,k**. This material is available free of charge via the Internet at <http://pubs.acs.org>.

■ AUTHOR INFORMATION

Corresponding Author

*E-mail: hatice.berber@univ-reims.fr.

Notes

The authors declare no competing financial interest.

■ ACKNOWLEDGMENTS

We thank C. Petermann and C. Machado for spectroscopic recordings (NMR and MS, respectively), S. Lanthony for microanalysis and HPLC technical assistance, and CNRS, PLANET for financial support.

■ REFERENCES

(1) (a) Eliel, E. L.; Wilen, S. H. *Stereochemistry of Organic Compounds*; Wiley-Interscience: New York, 1994. (b) Wolf, C.

Dynamic Stereochemistry of Chiral Compounds; Royal Society of Chemistry: Cambridge, U.K., 2008. (c) Clayden, J.; Fletcher, S. P.; McDouall, J. J. W.; Rowbottom, S. J. M. *J. Am. Chem. Soc.* **2009**, *131*, 5331–5343. (d) Gustafson, J. L.; Lim, D.; Miller, S. J. *Science* **2010**, *328*, 1251–1255. (e) Gustafson, J. L.; Lim, D.; Barrett, K. T.; Miller, S. J. *Angew. Chem., Int. Ed.* **2011**, *50*, 5125–5129. (f) Leermann, T.; Broutin, P.-E.; Leroux, F. R.; Colobert, F. *Org. Biomol. Chem.* **2012**, *10*, 4095–4102. (g) Leroux, F. R.; Berthelot, A.; Bonnafoux, L.; Panossian, A.; Colobert, F. *Chem.—Eur. J.* **2012**, *18*, 14232–14236. (h) Ros, A.; Estepa, B.; Ramirez-Lopez, P.; Alvarez, E.; Fernandez, R.; Lassaletta, J. M. *J. Am. Chem. Soc.* **2013**, *135*, 15730–15733.

(2) (a) Clayden, J.; Moran, W. J.; Edwards, P. J.; LaPlante, S. R. *Angew. Chem., Int. Ed.* **2009**, *48*, 6398–6401. (b) LaPlante, S. R.; Edwards, P. J.; Fader, L. D.; Jakalian, A.; Hucke, O. *ChemMedChem.* **2011**, *6*, 505–513. (c) LaPlante, S. R.; Fader, L. D.; Fandrick, K. R.; Fandrick, D. R.; Hucke, O.; Kemper, R.; Miller, S. P. F.; Edwards, P. J. *J. Med. Chem.* **2011**, *54*, 7005–7022.

(3) (a) Cano, C.; Golding, B. T.; Haggerty, K.; Hardcastle, I. R.; Peacock, M.; Griffin, R. J. *Org. Biomol. Chem.* **2010**, *8*, 1922–1928. (b) Yoshida, K.; Itoyama, R.; Yamahira, M.; Tanaka, J.; Loac̄, N.; Lozach, O.; Durieu, E.; Fukuda, T.; Ishibashi, F.; Meijer, L.; Iwao, M. *J. Med. Chem.* **2013**, *56*, 7289–7301.

(4) (a) Takahashi, H.; Wakamatsu, S.; Tabata, H.; Oshitari, T.; Harada, A.; Inoue, K.; Natsugari, H. *Org. Lett.* **2011**, *13*, 760–763. (b) Tabata, H.; Nakagomi, J.; Morizono, D.; Oshitari, T.; Takahashi, H.; Natsugari, H. *Angew. Chem., Int. Ed.* **2011**, *50*, 3075–3079. (c) Moure, A.; Sanclimens, G.; Bujons, J.; Masip, I.; Alvarez-Larena, A.; Pérez-Payá, E.; Alfonso, I.; Messeguer, A. *Chem.—Eur. J.* **2011**, *17*, 7927–7939. (d) Paul, B.; Butterfoss, G. L.; Boswell, M. G.; Renfrew, P. D.; Yeung, F. G.; Shah, N. H.; Wolf, C.; Bonneau, R.; Kirshenbaum, K. *J. Am. Chem. Soc.* **2011**, *133*, 10910–10919. (e) Wakamatsu, S.; Takahashi, Y.; Tabata, H.; Oshitari, T.; Tani, N.; Azumaya, I.; Katsumoto, Y.; Tanaka, T.; Hosoi, S.; Natsugari, H.; Takahashi, H. *Chem.—Eur. J.* **2013**, *19*, 7056–7063. (f) LaPlante, S. R.; Forgiione, P.; Boucher, C.; Coulombe, R.; Gillard, J.; Hucke, O.; Jakalian, A.; Joly, M.-A.; Kukulj, G.; Lemke, C.; McCollum, R.; Titolo, S.; Beaulieu, P. L.; Stammers, T. J. *J. Med. Chem.* **2014**, *57*, 1944–1951.

(5) Tietze, L. F.; Schuster, H. J.; von Hof, J. M.; Hampel, S. M.; Colunga, J. F.; John, M. *Chem.—Eur. J.* **2010**, *16*, 12678–12682.

(6) Delaye, P.-O.; Lameiras, P.; Kervarec, N.; Mirand, C.; Berber, H. *J. Org. Chem.* **2010**, *75*, 2501–2509.

(7) For review articles on recent advances on CBD, see: Mechoulam, R.; Peters, M.; Murillo-Rodriguez, E.; Hanuš, L. O. *Chem. Biodiversity* **2007**, *4*, 1678–1692.

(8) Appendino, G.; Gibbons, S.; Giana, A.; Pagani, A.; Grassi, G.; Stavri, M.; Smith, E.; Rahman, M. M. *J. Nat. Prod.* **2008**, *71*, 1427–1430.

(9) (a) Ballerini, E.; Minuti, L.; Piermatti, O.; Pizzo, F. *J. Org. Chem.* **2009**, *74*, 4311–4317. (b) Wilkinson, S. M.; Price, J.; Kassiou, M. *Tetrahedron Lett.* **2013**, *54*, 52–54.

(10) (a) Tamir, I.; Mechoulam, R. *J. Med. Chem.* **1980**, *23*, 220–223. (b) Kane, V. V.; Martin, A. R.; Jaime, C.; Ōsawa, E. *Tetrahedron* **1984**, *40*, 2919–2927.

(11) (a) Mechoulam, R.; Shvo, Y. *Tetrahedron* **1963**, *19*, 2073–2078. (b) Uliss, D. B.; Razdan, R. K.; Dalzell, H. C. *J. Am. Chem. Soc.* **1974**, *96*, 7372–7374.

(12) (a) Tanaka, H.; Ichino, K.; Ito, K. *Chem. Pharm. Bull.* **1984**, *32*, 3747–3750. (b) Ichino, K.; Tanaka, H.; Ito, K. *Tetrahedron* **1988**, *44*, 3251–3260. (c) Ichino, K. *Phytochemistry* **1989**, *28*, 955–956.

(13) (a) Orjala, J.; Wright, A. D.; Erdelmeier, C. A. J.; Sticher, O.; Rali, T. *Helv. Chim. Acta* **1993**, *76*, 1481–1488. (b) Benosman, A.; Oger, J.-M.; Richomme, P.; Bruneton, J.; Sévenet, T.; Ito, K.; Ichino, K.; Hamid, A.; Hadi, A. *J. Nat. Prod.* **1997**, *60*, 921–924.

(14) (a) Bhayana, B. *J. Org. Chem.* **2013**, *78*, 6758–6762. (b) Clayden, J.; Worrall, C. P.; Moran, W. J.; Helliwell, M. *Angew. Chem., Int. Ed.* **2008**, *47*, 3234–3237. (c) Eto, M.; Yamaguchi, K.; Shinohara, I.; Ito, F.; Yoshitake, Y.; Harano, K. *Tetrahedron* **2010**, *66*, 898–903.

(15) *P, M* nomenclature can also be used in sp^2 – sp^3 axial chirality, and the conformers can be considered as epimers here; the other centres of chirality are not indicated in their numeral names for clarity.

(16) (a) Sandström, J. *Dynamic NMR Spectroscopy*; Academic Press: New York, 1982. (b) Shanan-Atidi, H.; Bar-Eli, K. H. *J. Phys. Chem.* **1970**, *74*, 961–963.

(17) Line-shape simulation was carried out using Topspin 2.1 Bruker program; see the Supporting Information for details.

(18) For full reference of Gaussian09 program; see the Supporting Information.

(19) (a) Peng, C.; Schlegel, H. B. *Isr. J. Chem.* **1993**, *33*, 449–454.

(b) Peng, C.; Ayala, P. Y.; Schlegel, H. B.; Frisch, M. J. *J. Comput. Chem.* **1996**, *17*, 49–56.

(20) Masson, E. *Org. Biomol. Chem.* **2013**, *11*, 2859–2871.

(21) (a) Foster, J. P.; Weinhold, F. *J. Am. Chem. Soc.* **1980**, *102*, 7211–7218.

(22) The strongest interactions obtained in the both cases (NBO and NMR) between OMe and C3-H may refer to intramolecular H-bonding and/or hyperconjugation between O lone-pair electrons and the antibonding C3-H orbital ($O_{lp} \rightarrow \sigma^*_{C3-H}$). A deep study (experimental and theoretical) on the exact nature of these interactions is in progress and a full discussion will follow in a later report.

(23) For the preparation of (*M,P*)-**11**, see procedures in (a) Thompson, A. L. S.; Kabalka, G. W.; Akula, M. R.; Huffman, J. W. *Synthesis* **2005**, *4*, 547–550. (b) Hirota, K.; Isobe, Y.; Maki, Y. *J. Chem. Soc., Perkin Trans. 1* **1989**, 2513–2514.